Spring 2021

Provenance of early Paleogene strata in the Bighorn Basin (Wyoming, U.S.A.): Implications for Laramide tectonism and basin-scale stratigraphic patterns

Jessica L. Welch
Western Washington University, welchj22@wwu.edu

Provenance of early Paleogene strata in the Bighorn Basin (Wyoming, U.S.A.): Implications for Laramide tectonism and basin-scale stratigraphic patterns

By

Jessica L. Welch

Accepted in Partial Completion
of the Requirements for the Degree
Master of Science

ADVISORY COMMITTEE

Dr. Brady Foreman

Dr. Nicole McGowan

Dr. Sean Mulcahy

GRADUATE SCHOOL

David L. Patrick, Dean

Master's Thesis

In presenting this thesis in partial fulfillment of the requirements for a master's degree at Western Washington University, I grant to Western Washington University the non-exclusive royalty-free right to archive, reproduce, distribute, and display the thesis in any and all forms, including electronic format, via any digital library mechanisms maintained by WWU.

I represent and warrant this is my original work, and does not infringe or violate any rights of others. I warrant that I have obtained written permissions from the owner of any third party copyrighted material included in these files.

I acknowledge that I retain ownership rights to the copyright of this work, including but not limited to the right to use all or part of this work in future works, such as articles or books.

Library users are granted permission for individual, research and non-commercial reproduction of this work for educational purposes only. Any further digital posting of this document requires specific permission from the author.

Any copying or publication of this thesis for commercial purposes, or for financial gain, is not allowed without my written permission.

Jessica L. Welch

05/26/2021

Provenance of early Paleogene strata in the Bighorn Basin (Wyoming, U.S.A.): Implications for Laramide tectonism and basin-scale stratigraphic patterns

A Thesis
Presented to
The Faculty of
Western Washington University

In Partial Fulfillment
Of the Requirements for the Degree
Master of Science

by
Jessica L. Welch
May 2021

Abstract

The Bighorn Basin (Wyoming, U.S.A.) contains some of the best exposed and studied nonmarine early Paleogene strata. Over a century of research has produced a highly resolved record of early Paleogene terrestrial climatic and biotic change as well as extensive documentation of spatiotemporal variability in basin-scale stratigraphy. The basin also offers the opportunity to integrate these data with the uplift and erosional history of the Laramide uplifts that surround the Bighorn Basin. Herein we provide a comprehensive provenance analysis of the early Paleogene Fort Union and Willwood formations in the Bighorn Basin from paleocurrent measurements (n = 510 measurements), detrital zircon U-Pb geochronology (n = 2,258 age determinations), and sandstone compositions (n = 76 thin sections) obtained from fluvial sand bodies distributed widely across the basin. We aim to address the following questions; why there are lithologic changes between the Fort Union and the Willlwood formations, why is there spatial variation of grain size within the Willwood formation, and does the boundary sandstone represent a greater efficiency of sediment transport or a change in provenance.

From these new data, and data compiled from previous studies (May et al, 2013) we are able to present a comprehensive paleodrainage and unroofing history for the Bighorn, Owl Creek, and Beartooth Mountains as well as identify hinterland sediment sources in the Sevier fold-and-thrust belt. Broadly, we observe data consistent with (1) erosion of latest Cretaceous shales from the Bighorn Mountains and westward transport into the basin; (2) erosion of Late Cretaceous shales as well as lower Mesozoic and upper Paleozoic siliciclastics from the Owl Creek Mountains and its transport north and northwest into the basin; and (3) erosion of lower Mesozoic sedimentary cover, Paleozoic sedimentary cover, and crystalline basement from the Beartooth Mountains eastward into the northern Bighorn Basin. Similar to previous studies, we find evidence for a system of transverse rivers contributing water and sediment to an axial river system that drained north into southern Montana during both the Paleocene and Eocene. Additionally, the data indicate asymmetric unroofing histories on either side of the Bighorn and Owl Creek mountains, implying a drainage divide that we attribute to the vergence direction of the underlying basement reverse faults and exacerbated by the prevailing paleoclimate. In the southwestern and northern portions of the basin we find evidence for (1) sediment sourced from the diverse Phanerozoic cover and the Neoproterozoic Brigham Group quartzites in the Paris thrust sheet of southeastern Idaho; (2) erosion of sediment from the Idaho Batholith; and (3) sediment likely generated from the crystalline basement of the Tobacco Root Mountains and Madison Range in Montana transported southward and eastward to the Bighorn Basin. We suggest this sediment was funneled through the hypothesized Monida transverse structural zone situated between the Helena and Wyoming salients of the Sevier fold-and-thrust belt, then into the Absaroka Basin, and across the Cody Arch into the Bighorn Basin. This provenance pattern appears to have largely continued until ~50 Ma at which point more proximal source areas were available in the Absaroka volcanic province.

Basin-scale patterns in the stratigraphy of the Fort Union and Willwood formations were a product of catchment size and the lithologies eroded from the associated highlands. Mudrock-dominated strata in the eastern and southeastern Bighorn Basin are inferred to be caused by comparably smaller catchment areas and the finer-grained Mesozoic strata eroded. The conglomeratic and sand-dominated strata of the southwestern area of the Bighorn Basin are inferred to be caused by large, braided fluvial systems with catchments that extended for hundreds of kilometers into the Sevier fold-and-thrust belt and erosion of more resistant source lithologies.

The northernmost early Paleogene strata represents the coalescing of these fluvial systems as well as rivers whose catchments extended into southwestern Montana that contained more resistant, crystalline lithologies. These factors generated the thick, laterally extensive fluvial sand bodies common in that area of the basin.

Acknowledgements

This work was funded by a grant through the Western Washington University Geology Department, a Geological Society of America Graduate Research Grant, a Colorado Scientific Society Grant, and the ISU Foundation and Keck Grants to D. Malone and J. Craddock in 2011 and 2012. Thank you to several individuals for assistance in the field and laboratory as well as discussions that improved this work. These individuals include M. Pecha, M. Strow, L. Stodden, D. Rasmussen, N. McGowan, S. Mulcahy, E. Lalor, and G. Sutherland. A special thank you to my advisor Brady Foreman, and my family, friends, and furry friends for the continuous support and encouragement.

Table of Contents

List of Tables and Figures

INTRODUCTION

During the Early and Late Cretaceous, the Rocky Mountain region was located in the Sevier foreland basin. Thin-skinned deformation in western Montana, Idaho, and Utah provided substantial volumes of sediment that filled the foreland basin in central and eastern Montana, Wyoming, Utah, and Colorado (DeCelles, 2004; Dickinson, 2004; Lawton, 2008). Starting in the Late Cretaceous the Sevier foreland basin was broken up by the onset of the Laramide Orogeny, characterized by thick-skinned deformation, that continued into the Eocene (DeCelles, 2004; Dickinson, 2004; Copeland et al., 2017). The sediment that was initially deposited within the Sevier foreland basin was exhumed and eroded off Laramide uplifts. In addition to the over lying sedimentary cover, the underlying Paleozoic and Proterozoic strata and crystalline basement of Archean and Proterozoic age were in part eroded off the Laramide uplifts. The Laramide Orogeny contributed to the regression of the Cretaceous Interior Seaway and provided new sediment sources for the foreland; it also produced intermontane, flexural basins, and altered the regional climate (DeCelles, 2004; Dickinson, 2004; Sewall & Sloan, 2006; Lawton, 2008). Herein, we focus on the Paleocene and earliest Eocene strata within the Bighorn Basin of northwest Wyoming and use an extensive provenance analysis to extract information on the history of Laramide deformation and influences on basin deposition.

This study is important because it provides a comprehensive paleodrainage analysis as well as addressing unroofing pattern of the Bighorn Mountains to the east, the Owl Creek Mountains to the south, and Beartooth Mountains to the northwest of the Bighorn Basin, and any extra-basinal sediment sources associated with the Sevier fold-and-thrust belt.

We utilized several complementary provenance techniques in this research. These include paleocurrent analysis, sandstone compositions, and detrital zircon U-Pb geochronologic analysis

of fluvial sand bodies from sites across the basin. Study areas include the eastern portion of the basin (west of the Bighorn Mountains), the southeast portion of the basin (near the junction between the Bighorn and Owl Creek Mountains), the southwest portion of the basin (near the Cody Arch proposed by Sundell, 1990), and the northern portion of the basin (east of the Beartooth Mountains). This data stratigraphically captures the Fort Union (Paleocene) and Willwood (Eocene) formations as well as the "Boundary Sandstone" (Paleocene-Eocene boundary). Basin-scale paleocurrent coverage constrains the flow directions of major paleo-rivers within the basin and the geographic locations of topographic highs. The detrital zircon geochronologic and thin section data permits assessments of the provenance of the Fort Union and Willwood formations temporally and spatially across the Bighorn Basin.

Laramide uplifts surrounding the Bighorn Basin contain exposures of Upper Cretaceous shales and fluvio-deltaic strata, Lower Cretaceous and Jurassic siliciclastic strata, Upper Paleozoic siliciclastic rocks, Paleozoic carbonate rocks, and Precambrian crystalline rocks. The sedimentary cover and crystalline basement have distinct detrital zircon geochronologic signatures. Additionally, extra-basinal sediment sources can be identified in the detrital zircon geochronologic datasets as well as conglomerate and sandstone composition. This study aims to gain a comprehensive paleodrainage analysis and provenance analysis along with unroofing pattern of mountains surrounding the Bighorn Basin and identify any extra-basinal sediment sources. The contributions of this work show evidence for transverse river systems that drained the Bighorn Mountains, Owl Creek Mountains, and Beartooth Mountains that contributed both water and sediment to a main axial river system, which ran north through the basin. Evidence for a drainage divide in the Bighorn and Owl Creek mountains during the Paleocene and Eocene that led to differing unroofing histories for the surrounding Laramide basins as compared to the Bighorn

Basin. Additionally, there is good evidence for input of sediment from the Sevier fold-and-thrust belt, Idaho Batholith, and western Laramide structures such as the Tobacco Root Mountains and Madison Range in southwestern Montana. This suggests that during the Paleocene and-widespread lacustrine deposition of the early Eocene these western hinterlands continued to be important during alluvial deposition in Laramide basins (Davis et al., 2010; Chetel et al., 2011; Craddock et al., 2015; Malone et al., 2017). Finally, the provenance histories, drainage patterns, and inferred differences in relative catchment sizes appear to play a first order control on basin-scale stratigraphic patterns in the Fort Union and Willwood formations.

GEOLOGIC HISTORY

Tectonic Setting

The Bighorn Basin is located in northwestern Wyoming and is bounded on three sides by Laramide uplifts (Fig. 1). The uplifts that bound the basin are the Beartooth Mountains to the northwest, the Pryor and Bighorn Mountains to the northeast and east, and the Owl Creek Mountains to the south. Thermochronologic and structural data suggest activity along several of the basement-involved reverse fault started in the Cretaceous and early Paleocene (Omar et al., 1994; Crowley et al., 2002; Peyton et al., 2012; Carrapa et al., 2019). Recent paleoseismic records suggest the effect of flat slab subduction at the western margin of North America may have affected the region as early as 82.4 to 78.0 Ma (Jackson et al., 2019). The major imbricate faults causing uplift are largely vergent to the east and northeast for the Beartooth, Pryor, and Bighorn mountains, and to the south for Owl Creek Mountains (Palmquist, 1978; Stearns & Stearns, 1978; DeCelles et al., 1991; Hoy & Ridgway, 1997). The broad effect of movement on these faults was the generation of hanging wall anticlines (drape folds) that involved the Archean basement and overlying Paleozoic and Mesozoic strata (Palmquist, 1978; Stearns & Stearns, 1978; DeCelles et al., 1991). From bottom to top, this sedimentary cover includes the Cambrian shallow marine units (i.e., Flathead Sandstone and Gros Ventre Formation), Paleozoic carbonates including the Bighorn Dolomite and Madison Limestone, upper Paleozoic siliciclastic units (i.e., Gallatin Group, Amsden Formation, Tensleep Sandstone, Phosphoria Formation), and a variety of Mesozoic siliciclastic units that include the Triassic Chugwater Formation, Sundance Formation, Jurassic Morrison Formation, Lower Cretaceous Cloverly Formation, Thermopolis Shale, Mowry Formation and Upper Cretaceous Mesa Verde Formation, Meeteetse Formation, Lewis Shale, and the uppermost Cretaceous Lance Formation). River systems draining the Laramide structures

received their sediment load from these geologic units. The potential source lithologies can be classified into groups with distinct detrital zircon U-Pb age spectra signatures (May et al., 2013; described in detail in the Discussion). Additionally, there have been suggestions for a strong extra-basinal influence on the tectonic evolution of the Bighorn Basin. This inference centers on the input of quartzite-rich conglomeratic braided river deposits along the southwest margin of the basin, which are hypothesized to have origins in southeastern Idaho or along the border of Idaho and southwestern Montana, and are linked to pulses of tectonism in the hinterland (Kraus, 1982; Janecke et al., 2000; Malone et al., 2017). The validity of these interpretations partially rests on the Absaroka Basin (now obscured by the Absaroka Volcanics) and paleotopographic expression of the Cody Arch that delimits the western margin of the Bighorn Basin. Later, during the Eocene volcanism associated with the Absaroka Range in the southwestern corner of the basin became important and likely influenced the generation of several large gravitational collapse structures such as the Heart Mountain Slide in ~49 Ma (Malone et al., 2014; 2017).

Paleogene Deposition

The Paleocene and Eocene Fort Union and Willwood formations, are exposed across much of the basin (Fig. 1). The Fort Union Formation is exclusively Paleocene in age, varies in thickness from 600 meters in the southeast to over 3000 meters in the north, and was deposited by fluvial systems with poorly drained floodplains and intervals of lacustrine, at times swampy, deposition (Fig. 2C and D) (Bown, 1980a; Hickey, 1980; Yuretich et al.,1984; Gingerich, 2001; Foreman, 2014). The Fort Union Formation overlies the Cretaceous Lance Formation, and the contact

between the two formations is typically expressed as a slight angular unconformity (Bown, 1980a). The Fort Union Formation consists of a variety of rock types, sandstone, siltstone and mudstone with lesser amounts of limestone, coal, carbonaceous shale, and conglomerates (Hickey, 1980; Rice et al., 2008; Gao & Fan, 2018). The mudstones, shales and paleosols have a distinctive drab grey, green, and purple coloring, while the carbonaceous shales and coal are a dark grey color (Hickey, 1980). Sand bodies can be lenticular or sheet-like in geometry and display average thicknesses of 6 m and width of 1 km and contain sedimentary structures like dune and ripple cross-stratification, and broadly fine upwards (Hickey, 1980; Foreman, 2014; Owen et al., 2017). These sand bodies are interpreted as fluvial in origin, and commonly contain multiple scour surfaces and stories indicating channel mobility and avulsion reoccupation events (Hickey, 1980; Foreman, 2014; Owen et al., 2017). These fluvial sand bodies are relatively common at the southwestern, western, and northern exposures within the Bighorn Basin and associated with drab overbank facies indicative of poorly drained floodplains (Hickey, 1980). Exposures of the Fort Union Formation along the eastern margin of the basin are generally fine-grained with comparatively fewer large fluvial sand bodies. The northernmost basin strata and exposures in southern Montana contain more abundant paludal and lacustrine facies, suggesting fluvial systems emptied into large, shallow lake systems (Hickey, 1980).

The Willwood Formation overlies the Fort Union Formation conformably, disconformably, and in some locations at an angular unconformity. Conformable successions occur closer to the basin center and disconformable successions along the basin margin, proximal to Laramide uplifts. The formation varies in thickness from ~750 m thick in the south to ~1500 m in the north. The formation contains fluvial and well-drained overbank deposits (Fig. 2A and B). The base of the Willwood Formation is defined by the lowest laterally continuous red bed, which

is time-transgressive across the basin (Kraus & Riggins, 2007). In the southern and southeastern Bighorn Basin, the transition between the Fort Union and Willwood formations occurs coincident with the Paleocene-Eocene (P-E) boundary. In the southwest the contact post-dates the P-E boundary, and in the northern basin the formational contact is older than the P-E boundary (Kraus, 1982; Wing et al., 2005; Kraus & Riggins. 2007). The Willwood contains both lenticular and sheet sandstones, heterolithic overbank strata, and paleosols that display a range of colors, most notably red, purple, and orange (Van Houten, 1944; Neasham & Vondra, 1972; Bown, 1980b; Bown & Kraus, 1981; Kraus, 1996; Kraus et al, 2015). The sheet sand bodies are as much as 30 m thick and several km wide perpendicular to flow, although typically they are ~10 m thick and 1 km wide and contain multiple stories (Foreman, 2014; Owen et al., 2017). Within the sand bodies fining upward lithofacies associations are common which is consistent with meandering river facies models (Kraus & Aslan, 1993; Kraus & Middleton, 1987; Foreman, 2014; Owen et al., 2017). Lenticular sand bodies are interpreted as isolated meandering river channels and floodplain channels (Kraus & Middleton, 1987; Owen et al., 2017). Overbank strata include heterolithic "avulsion" deposits of tabular sandstones with ripple cross-laminations and bioturbation interpreted as crevasse splay sequences, and variegated mudrocks containing abundant carbonate nodules, mottles, and ped structures interpreted as well-drained floodplain soils (Kraus & Middleton, 1987; Kraus, 2001; Kraus & Riggins, 2007). Amalgamated, multi-storied fluvial sheet sand bodies are more common within the western and northern portions of the Willwood Formation exposures and isolated, lenticular sand bodies in the eastern portions of the basin (Kraus & Middleton, 1987; Kraus, 2001; Bown, 1980; Owen et al., 2017).

Spatial Variability in the Fort Union and Willwood Formations

There are distinct conglomeratic units in both the Fort Union and Willwood formations. On the western margin of the Bighorn Basin along the Beartooth Mountains are exposures of the Beartooth Conglomerate (Fig. 2F). The Beartooth Conglomerate is an upper Paleocene unit that was deposited by alluvial fans and coarse bedload-dominated streams (Flueckinger, 1970; Neasham and Vondra, 1972; Jobling, 1974; Dutcher et al., 1986; DeCelles et al., 1989; 1991). This unit has an exposed thickness of ~730 m along the northern side of Clark's Fork Canyon Road (DeCelles et al. 1991). The conglomerate facies interfingers with the Paleocene Fort Union Formation as it grades laterally towards the central Bighorn Basin. Eocene-aged alluvial fan deposits are not present adjacent to the Beartooth Mountains, however, these may have been eroded during post-Miocene excavation of the Bighorn Basin, as the Beartooth Conglomerate is the youngest stratigraphic unit. The Beartooth Conglomerate exhibits a clear unroofing history, and several studies have examined the structural and thermochronologic evolution of the Beartooth Mountains (Flueckinger, 1970; DeCelles et al., 1989; 1991; Omar et al., 1994; Peyton et al., 2012; Carrapa et al., 2019).

Additionally, thick, sheet-like, quartzite-rich conglomeratic units crop out in the southwestern portion of the basin near the town of Meteetsee, Wyoming. These occur in both the Fort Union and Willwood formations and are interpreted as braided fluvial units (Neasham & Vondra, 1972; Kraus, 1982; 1985; Seeland, 1998; Owen et al., 2017; Malone et al, 2017). In contrast, there is a notable absence of similar alluvial fan and braided river deposits along the eastern and southeastern margin of the Bighorn Basin, adjacent to the Bighorn and Owl Creek Mountains (Bown, 1980a,b; Owen et al., 2017). Instead these areas are dominated by clay and siltstone overbank lithfacies as well as cut-and-fill structures (Bown, 1994; Kraus, 1980; Kraus,

1992; Kraus, 1996; Wing et al., 2005; Owen et al. 2017). These cut-and-fill structures are lenticular in geometry with distinct scour surfaces filled with silt to fine sand units, typically massive and in some cases rippled or trough cross-bedded. These have been interpreted as suspended load meandering rivers (Kraus, 1980; Kraus, 1992; Kraus, 1996; Wing et al., 2005; Owen et al. 2017).

Paleocene Eocene Thermal Maximum and the "Boundary Sandstone"

The Paleocene-Eocene Thermal Maximum (PETM) was a global warming event that occurred 56 Ma and lasted approximately 200,000 years (Kennett and Stott, 1991; Westerhold et al., 2009; Murphy et al., 2010; Cui et al., 2011). The PETM has been extensively studied using geochemical proxies in the Bighorn Basin and is identified by an abrupt negative stable carbon isotope excursion in soil carbonate nodules and fossil plant matter (Koch et al., 1992; Bowen et al., 2001; Wing et al., 2005; Smith et al., 2007; Baczynski et al., 2013). This negative carbon isotope excursion can be found in both marine and terrestrial strata globally (Koch et al., 1992; Zachos et al., 1993, 2005; McInerney and Wing, 2011), and is thought to be due to the release of isotopically-light carbon into Earth's oceans and atmosphere; perhaps >4000 petagrams (Pg) of carbon ultimately derived from methane clathrates previously hosted in the ocean sediments (Murphy et al., 2010; McInernery & Wing, 2011). The carbon isotope excursion is associated with an increase in global temperatures by about 5 °C in less than 10,000 years, which is also reflected in proxies from the Bighorn Basin (Fricke et al., 1998; Wing et al., 2005; Murphy et al., 2010; McInernery & Wing, 2011). Soil geochemistry and plant fossils suggest that mean annual precipitation decreased by ~40% during the PETM (Wing et al., 2005; Kraus and Riggins, 2007; Kraus et al., 2015). Studies of paleosols (Kraus and Riggins, 2007; Adams et al., 2011; Kraus et al., 2015) and paleosol ichnofossils (Smith et al., 2008) suggest that there were drier conditions

associated with the onset of the PETM, but fluctuations in the water table potentially indicate more seasonal conditions.

The "Boundary Sandstone" (also called the Clarks Fork sandstone of Kraus (1980)) is a thick and laterally continuous fluvial sand body located at the Paleocene-Eocene boundary in the northern Bighorn Basin (Kraus, 1980; Foreman, 2014; Kraus et al., 2015). This sandbody also marks the boundary between strata that contain Clarkforkian-age mammal fossils and strata that contain mammalian fossils of Wasatchian age (Rose, 1978. 1979; Gingerich et al., 1980). Carbon isotope records spanning the Boundary Sandstone indicate it is located within the PETM (Foreman, 2014). The sandbody can locally reach thicknesses in excess of 30 m and can be traced laterally for >10 km (Kraus, 1980; Foreman, 2014). This makes the multi-storied sand body anomalously thick and laterally persistent compared to other fluvial sandbodies in the northern basin, and it has been interpreted to have been caused by greater channel mobility and sediment transport efficiency during the PETM (Foreman, 2014; Kraus et al., 2015). However, previous studies did not constrain provenance patterns straddling the Boundary Sandstone, which leaves a key hypothesis for its generation largely untested. Namely, that the Boundary Sandstone is due to a coarsening of the sediment caliber provided to the basin related to unroofing of a different lithology in the source area. This Boundary Sandstone appears to be a unique response in the northern Bighorn Basin, as there is no equivalent in the southern and south-central Bighorn Basin where the PETM has been identified (Wing et al., 2005; Kraus & Riggins, 2007; Baczynski et al., 2013). The PETM strata near Worland, Wyoming, show a shift to thicker and more well-developed paleosols and the generation of cut-and-fill lenticular bodies (Wing et al., 2005; Kraus and Riggins, 2007; Baczynski et al., 2013).

METHODS

Paleocurrent Analysis

Drainage patterns were reconstructed using paleocurrent measurements derived from large- and small-scale trough and planar cross-stratification in fluvial sand bodies (Fig. 3A, B). These sedimentary structures preserve the remnants of dunes that, in aggregate, migrate downstream (Potter & Pettijohn, 1977). The paleocurrents presented herein encompass new data and vector mean directions from previous studies (Neasham and Vondra, 1972; DeCelles et al., 1991; Seeland, 1998; Foreman, 2014). In most cases data are divided broadly into the Fort Union and Willwood formations, but the data can be further sub-divided by mammalian biozones in some study areas, as noted in the text.

No new paleocurrent measurements were made in the eastern study area of the basin as both Neasham & Vondra (1972) and Seeland (1998) report extensive data in that area. In the southeastern portion of the Bighorn Basin, paleocurrent directions were determined from the Fort Union Formation (n = 37; restricted to the Clarkforkian biozone) and Willwood Formation (n = 49; spanning Wasatchian 1-6 biozones). In the southwestern portion of the basin the biostratigraphic constraints are weaker and paleocurrent measurements were broadly binned into the upper Fort Union Formation (n = 10; Paleocene) and Willwood Formation (n = 34; Eocene). In the western Bighorn basin new paleocurrents were measured from the Fort Union Formation (n = 9; Paleocene) and Willwood Formation (n = 24; Eocene). Paleocurrent measurements from the northern Bighorn Basin presented here represent a compilation of prior (n = 353; Foreman, 2014) and new (n = 37) measurements that span mammal biozones Tiffanian-1 through Wasatchian-7 biozones. This comprehensive paleodrainage analysis allows for tracking of secular shifts in river

flow and aids in identifying which Laramide uplifts may have been uplifting and thus increasing paleo-slopes. These paleocurrent data were used to produce rose diagrams of the paleocurrents from the north, east, west, southeast and southwest.

Fluvial Sandstone Composition

The compositions of sandstones were point-counted under a petrographic microscope as a complementary provenance tool for detrital zircon U-Pb geochronologic. Medium-grained fluvial sandstones were sampled from the Fort Union and Willwood formations, including those associated with the PETM. A total of 76 samples were collected and thin sectioned (Fig. 1). In the eastern study area, two samples were collected, one from each of the Fort Union and Willwood formations. Thirteen samples were collected from the southeastern region of the basin. Seven samples are from the Fort Union Formation, six from the Willwood Formation, and one from the thin, grit pebble conglomerate associated with the onset of the PETM identified by Wing et al. (2005). In the southwest region thirteen samples were collected. Five samples are from the Fort Union Formation, and eight samples are from the Willwood Formation. Forty-three samples were collected from the northern Bighorn Basin. Nine samples are from the Fort Union Formation, seven from the PETM interval, and 27 from the Willwood Formation. These samples can be further sub-divided by mammal biozones of the Tiffanian (n = 4); the Clarkforkian (n = 5); a combined Wasatchian M and 0 biozone that encompasses the PETM (n = 7); the combined Wasatchian 1 through 4 biozones (n = 7); the combined Wasatchian 5 and 6 (n = 17); and the Wasatchian 7 biozone (n = 3). Additionally, two samples were collected from the Beartooth Conglomerate in the very northwestern portion of the basin, both are Clarkforkian in age (Fig. 1; DeCelles et al., 1991).

Sandstone samples were impregnated with epoxy, cut, ground, and polished to 30 μm thickness on glass thin sections. Thin sections were stained with Na-cobaltinitrite and K-

rhodizionate to aid in identification of K-feldspar and plagioclase, respectively. Sandstone compositions were determined using Gazzi-Dickinson point-counting methodology with a transmitted-light microscopy (Dickinson, 1970; Dickinson and Suczek 1979; Dickinson et al., 1983; Ingersoll et al., 1984). Five hundred sand-sized detrital grains were identified and counted for each thin section. Pores, cement, and matrix were not counted. Total counts were tabulated into quartz, feldspar, and lithic categories and plotted as poles on ternary classification diagrams (Folk, 1980; Dickinson, 1985). Using these data ternary diagrams that were sub-divided by formation and geographic area were produced.

U-Pb Detrital Zircon Geochronology

Fluvial sand bodies in the Willwood and Fort Union formations were sampled at several locations and stratigraphic positions across the Bighorn Basin to obtain a detrital zircon U-Pb geochronologic dataset. Eighteen new samples were analyzed and three were compiled from May et al. (2013). The data span mammal biozones Tiffanian-3 to Wasatchian-7, but these biozones were not all sampled at each study area. The dataset represents 2,276 new and 295 compiled U-Pb age determinations with an average number of age determinations per fluvial sand body sampled of 132. This was calculated by adding together the number of age determinations each sample had and then dividing by the total number of samples to get the average number of age determinations per fluvial sand body sampled.

U-Pb ages were determined at the LaserChron laboratory at the University of Arizona, Tucson AZ, using a Nu high resolution-multicollector-inductively coupled plasma-mass spectrometer (HR-MC-ICP-MS) coupled to a Photon Machines Analyte G2 laser ablation system. Samples were prepared using standard methods outlined by the Arizona Laserchron Center (http://www.laserchron.org; Gehrels et al. 2008; Gehrels and Pecha 2014). Separated zircons

grains were mounted with fragments of the Sri Lanka standard (U-Pb age 563.5 ± 3.2 Ma) (Gehrels et al. 2008) in epoxy and polished. Detailed information on run parameters and procedures can be found in Gehrels and Pecha (2014). The Sri Lanka standard was analyzed between every five unknown analyses (Gehrels et al., 2008). Unknown analyses were corrected for background, ^{204}Pb ("common" lead), and fractionation, with uncertainties in these corrections, the Sri Lanka standard uncertainties, and the uncertainties associated with the decay constants for ^{238}U and ^{235}U all propagated to the final reported age. "AgeCalc" was used for data reduction to determine the age, uncertainty, discordance etc. (Gehrels and Pecha, 2014). A conservative 10% discordance filter was applied to both new and compiled ages similar to previous studies done by Gehrels and Pecha, 2014 and May et al. 2013. Measurement error was 1-2% (2σ), and the normalized age spectra frequency distributions include an assumption of normal distribution around the standard deviation of the age error for each grain age. Peak ages were determined by a minimum of three overlapping ages. (Gehrels et al. 2006; Gehrels et al. 2008)

Early Paleogene strata age peaks and their relative magnitudes were compared to assess secular provenance changes. Identification of specific source lithologies was performed through comparison with known age spectra of Mesozoic and Paleozoic strata exposed along the margins of the Bighorn Basin (May et al., 2013) and the ages of crystalline basement in the region (Gast et al., 1968; Frost & Fanning, 2006). Normalized probability density plots were produces from these data for the Fort Union and Willwood formation.

RESULTS

Paleocurrent Analysis Results

The new paleocurrent data are presented here and interpreted with other studies paleocurrent data (Fig. 1 and Fig. 3C). In the southeast the paleocurrents for the Fort Union and Willwood formations are directed more towards west and northwest. The vector mean paleocurrent direction from the Fort Union Formation is 271° (n = 37) and the Willwood Formation is 349° (n = 49). In the southwestern study area, both the Fort Union Formation and Willwood Formation paleocurrents show drainage slightly towards a northeast trend. The vector mean paleocurrent direction for the Fort Union Formation is 34° (n = 12) and the vector mean for the Willwood Formation is 33° (n = 34). The vector mean paleocurrent direction for the western study area for the Fort Union Formation is 357° (n = 9) while the Willwood Formation is 340° (n = 24). However, these are relatively small sample sizes and must be integrated into the broader paleodrainage database (Fig. 3C). In the northern study area of the basin both the Fort Union and Willwood formations show a strong paleodrainage direction towards the north with a vector mean direction of 359° for the Fort Union Formation (n = 95 measurements) and 342° for the Willwood Formation (n = 137). The Boundary Sandstone associated with the PETM shows a vector mean of 128° (n = 100).

Fluvial Sandstone Composition

Results for sandstone petrographic analyses are summarized in Table 1 and plotted in Fig. 4 and 5. Overall the Fort Union Formation and Willwood Formation sandstones are subarkoses and sublitharenites based on the Folk (1980) classification. The southeastern samples are mostly sublitharenites with a few subarkoses (Fig. 4). The southwest samples are subarkose and sublitharenite (Fig. 4). In the northern samples are variable in sandstone composition (Fig. 4)

ranging from arkose, to lithic arkose, subarkose, and sublitharenite. However, both the Fort Union and Willwood formation samples in the northern Bighorn Basin are lithic arkose (Table 1). Sandstone samples from the Beartooth Conglomerate in the northern Bighorn Basin are also lithic arkose (Fig. 4; Table 1).

Overall, the compositions of Fort Union and Willwood formation sandstones are similar within the north, east, southeast and southwest study areas. The eastern, southeastern, and southwestern study areas are more quartz-rich as compared to the northern samples (Fig. 4; Table 1). The QpLvLs plot show that the eastern, southeastern, and southwestern study areas are rich in sedimentary lithic fragments (Fig. 5). However, samples in the northern study area have a greater proportion of volcanic rock fragments and an increase in polycrystalline quartz as well as plagioclase (Fig. 5; Table 1). The exception in the northern study area is the Beartooth Conglomerate, which shows a greater proportion of sedimentary lithic fragments similar to sandstones in the other study areas.

In the northern study area, the sandstone samples were further divided by biozones to evaluate any up-section changes in mineralogy. From the Tiffanian samples to Wasatchian-4 samples there is a progressive reduction in the percentage of quartz and lithic fragments and an increase in the percentage of feldspar grains (Fig. 4). Samples from the Wasatchian 5-6 biozones and Wasatchian-7 biozone then show a return to higher percentages of quartz and lithic fragments (Fig. 4). Figure 5 suggests that these up-section changes did not generally co-occur with shifts in the relative proportions of polycrystalline, sedimentary lithics, and volcanic lithics. Wasatchian-7 samples are an exception and show a higher percentage of volcanic rock fragments compared to other samples in the northern study area (Fig. 5; Table 1).

U-Pb Detrital Zircon Geochronology

Detrital zircon geochronologic results are presented within the context of continental-scale primary sources that have been established by numerous previous studies (e.g., Dickinson & Gehrels, 2003; Dickinson & Gehrels, 2008; Gehrels et al., 2011; Laskowski et al., 2013). In this study we take a conservative approach to identify sediment provenance since substantial recycling of zircons from Paleozoic and Mesozoic sedimentary strata is expected in addition to the primary first-generation zircons from the crystalline basement. As such, we first present the relative abundance of zircon ages in our samples that fall within North American primary source ranges, and then outline the presence/absence of specific, diagnostic age peaks important for constraining provenance.

The important primary zircon age ranges that the data are divided into include: the coastal Cordilleran magmatic arc (CCM) 60-125 Ma, the interior Cordilleran magmatic arc (ICM) 130-205 Ma, the Appalachian-Ouachita orogen (AOO) 300-700 Ma, Grenville province (GP) 980-1300 Ma, anorogenic plutons (AP) 1300-1500 Ma, Yavapai-Mazatzal province (YMP) 1600-1800 Ma, the northern Laurentian province (NLP) 1800-2500 Ma and the Wyoming/Hearne/Rae craton (WHR) 2500-3220 Ma. Table 2 shows a summary of the different peaks identified in the samples within this study and their correspondence to these age populations as well as a summary of the relative percentages of zircon grain age determinations that fall into each of these primary source age ranges.

The single sample taken from the Willwood Formation in the eastern Bighorn Basin shows an age range of 74.4 ± 0.8 to 2937.4 ± 10.2 Ma (Fig. 6). The percentage of detrital zircon age grains that fall into each primary source range are as follows: CCM 31%, ICM 2%, MNM 0%, AOO 3%, GP 11%, AP 4%, YMP 31%, NLP 6% and WHR 7%. Within the CCM population,

there is a small peak at ~75 Ma in comparison to larger peaks at 93, 97, and 106 Ma (Fig. 6), and that this sample has the highest percentages of CCM and YMP grains and lowest percentage of WHR grains among all the samples.

The Willwood Formation in the southeastern Bighorn Basin shows an age range from 72.4 ± 1.4 to 3164.8 ± 19.4 Ma from one sample (Fig. 6). The percentage of age determinations that fall into each primary source are as follows: CCM 24%, ICM 1%, MNM 0%, AOO 3%, GP 9%, AP 8%, YMP 28%, NLP 12% and WHR 12%. The high percentage of YMP is similar to the Willwood formation in the eastern study area and the number of grains contributing to the 75 Ma peak compared to the 90 and 96 Ma peaks is low (Fig. 6). This sample shows a doubling of AP, NLP, and WHR percentages at the expense of CCM grains (Table 2).

In the southwest Bighorn Basin, the Fort Union Formation showed an age range of 67.4 ± 7 to 2790.9 ± 32.6 Ma (Fig. 6). The Willwood Formation from this area showed an age range from 81.3 ± 1.6 to 2549.2 ± 86.2 Ma. The proportions of detrital zircon ages in each primary source for the Fort Union Formation are as follows: CCM 35%, ICM 0%, MNM 0%, AOO 3%, GP 8%, AP 6%, YMP 19%, NLP 14%, and WHR 14%. The Willwood shows similar proportions; CCM 24%, ICM 2%, MNM 3%, AOO 6%, GP 14%, AP 9%, YMP 17% NLP 11% and WHR 12%. Major differences between the two formations are a higher percentage of CCM grains in the Fort Union Formation than in the Willwood Formation, and AOO and GP ages that are twice as prevalent in the Willwood Formation. Similar to the eastern and southeastern Willwood Formation study areas, the relative to proportion of grains that contribute to the ~70 Ma peaks compared to the ~98 Ma peaks is low (Fig. 6). The broad WHR peak for both the Fort Union and Willwood formations in the southwestern study area is centered at 2.7 to 2.8 Ga (Fig. 6).

In the northern study area of the Bighorn Basin, the pooled Fort Union Formation samples have an age range of 60.9 ± .7 to 3782.5 ± 10.1 Ma, and the pooled Willwood Formation shows an age range of 67.8 ± .7 to 3713.4 ± 8.5 Ma (Fig. 6). Overall, the Fort Union and Willwood in the north show similar patterns in the age spectra with a few key differences when compared to the other study areas (Fig. 6). The northern Fort Union Formation displays the following percentages of grains within the primary source ranges: CCM 21%, ICM 2%, MNM 1%, AOO 5%, GP 14%, AP 7%, YMP 14%, NLP 11% and WHR 20% of the detrital zircon age determinations. In the Willwood Formation we find the following percentages: CCM 24%, ICM 2%, MNM 2%, AOO 5%, GP 13%, AP 7%, YMP 14%, and the WHR 22% of the detrital zircon age determinations. Thus, on the formation-scale, the Fort Union and Willwood formations are very similar. Overall, the relative abundance of YMP grains is lower and the abundance of WHR grains is higher in the northern study area for both the Fort Union and Willwood formations as compared to other study areas. Additionally, the size of the ~75 Ma peak and ~98 Ma peak are comparable to one another, and there is a significant peak at ~2.5 Ga and ~3.3 Ga. All three of these features are different from the other study areas in the basin.

The Beartooth Conglomerate samples from the northern margin of the basin show an age range of 100 ± 1.8 to 3250.1 ± 3.9 Ma. The percentage of each primary source is as follows: CCM 1%, ICM 0%, MNM 0%, AOO 3%, GP 31%, AP 10%, YMP 24%, NLP 14% and WHR 11%. Thus, in comparison to other study areas the Beartooth Conglomerate displays a notable lack of CCM grains and an anomalously percentage of high GP (Fig. 6; Table 2). The single grain in the CCM yield an age of 100 ± 1.8 Ma. Additionally, Beartooth Conglomerate shows a greater abundance of YMP and lower abundance of WHR grains as compared to the Fort Union and Willwood formations in the northern study area.

In the northern Bighorn Basin detrital zircon samples were also examined by mammal biozone ranging from Tiffanian through Wasatchian. These were divided into 5 groups: (1) Tiffanian 3-4; (2) Tiffanian-6/Clarkforkian 2-3; (3) Wasatchian-M/0, (4) Wasatchian 1-5 (lower Wa-5 biozone); and (5) Wasatchian-5/6 (uppermost Wa-5 biozone) through 7 (Fig. 7). The Tiffanian 3-4 group showed an age range of 60.9 ± .7 to 3430.1 ± 30.8 Ma. Detrital zircons in this group show the following percentages: CCM 20%, ICM 2%, MNM 1%, AOO 6%, GP 15%, AP 8%, YM 18%, NLP 9% and WHR 18%. The Tiffanian-6/Clarkforkian 2-3 group ranges from 69.0 ± 2.3 to 3782.5 ± 10.1 Ma. The percentages that fall within the primary sources are as follows: CCM 22%, ICC 2%, MNM 2%, AOO 4%, GP 13%, AP 6%, YMP 9%, NLP 14%, and WHR 24% of the detrital zircon age determinations. The Wasatchian-0/M group, which includes the PETM Boundary sandstone, shows an age range of 67.8 ± .7 to 3713.4 ± 8.5 Ma. The percentages of each primary sources seen in this group are as follows; CCM 23%, ICM 3%, MNM 0%, AOO 7%, GP 16%, AP 7%, YM 12%, NLP 10% and WHR 17%. The Wasatchian 1-5 group has an age range of 68.1 ± 6.2 to 3658.9 ± 1.5 Ma and detrital zircons from this group show the following percentages: CCM 42%, ICM 1%, MNM 3%, AOO 5%, GP 12%, AP 7%, YM 10%, NLP 7% and WHR 10%. Lastly, the Wasatchian 5/7 through 7 group has an age range of 72.6 to 3363.7 Ma, and we found that percentage of age determinations that fell within the primary source age range are as follows: CCM 12%, ICC 1%, MNM 2%, AOO 4%, GP 11%, AP 6%, YMP 20%, NLP 8% and WHR 34%. Overall there are no dramatic up-section patterns in the age spectra. There is a shift to a greater abundance of grains ~75 Ma compared to peaks ~98 Ma starting in the Wasatchian 0/M biozone and continuing up-section. Additionally, the Wasatchian 1-4 group has significantly higher percentage of CCM grains and lower WHR grains compared to other biozones, and the Was 5/6 through 7 has the lowest CCM and highest WHR percentages.

DISCUSSION

Sediment Provenance & Laramide Tectonism

The location of significant topographic highs are deduced from paleocurrent data, as the aggregated direction of cross-stratification is directed downstream. In the eastern margin of the Bighorn Basin, paleodrainage was directed dominantly to the northwest and north with some areas showing more westward-directed paleoflows (Fig. 3C; Neasham & Vondra, 1972; Seeland, 1998). There does not seem to be a significant difference between the Fort Union and Willwood formation drainage patterns, and the data imply that the Bighorn Mountains were a topographic high during the Paleocene and Eocene. This is further supported by thermochronolgy data from the Bighorn mountain obtained by Crowley et al, (2002). In the southern portion of the basin, the paleodrainage direction for both formations is to the north, away from the Owl Creek Mountains (Fig. 3C). In the southwestern area of the basin, paleodrainage is directed to the northeast overall in both the Fort Union and Willwood formations, and eventually directed more northward for both formations (Fig. 3C). The development of the Absaroka volcanic province post-dates the Fort Union and Willwood formation studied herein (Smedes & Prostka, 1972; Sundell, 1993; Feeley & Cosca, 2002; Malone et al, 2014) suggesting a more distal, extra-basinal sediment source to the west. However, the Absaroka Volcanics do become an important sediment source later in the middle Eocene (Malone et al., 2014a, b; Malone et al., 2017b). Previous studies have documented paleocurrents from the Beartooth Conglomerate directed towards the east and northeast, and it appears these systems merged with northward-flowing river system within the basin center (DeCelles et al., 1991; Foreman, 2014; Fig. 9). Overall the paleocurrent data broadly outline two systems of rivers on the eastern and southwestern areas of the basin that merged near the basin center to drain north, where

an additional system of rivers draining the Beartooth Mountains added their sediment (Fig. 3C; 9). This pattern is consistent with previous proposals of a system of transverse rivers draining the Bighorn, Owl Creek, and Beartooth Mountains as well as an extra-basinal sediment source that combine into an axial river system that exits the basin into southeastern Montana. With this paleodrainage framework established, it is possible to interprete source lithologies for sediment using sandstone compositions and detrital zircon U-Pb geochronology data.

May et al. (2013) grouped the Phanerozoic sedimentary strata in the Bighorn Basin into four tectonostratigraphic assemblages (TSA1, TSA2, TSA3) based on lithologic characteristics and similar detrital zircon signatures, which are presented in Figure 8. These assemblages capture the major tectonic evolution of the area from a passive margin system for most of the Paleozoic, a transition period to a retro-arc foreland basin during the earliest Mesozoic, a retro-arc foreland basin during much of the Mesozoic generated by the Sevier Orogeny, and finally a broken foreland during the early Paleogene due to the Laramide Orogeny (May et al., 2013). May et al. (2013) note that TSA4 includes the Fort Union and Willwood formations and documents the erosion and redeposition of previous Phanerozoic strata captured in TSA1, TSA2, and TSA3, but they did not have the spatial coverage across the basin to discern unroofing histories for the various mountain ranges nor the stratigraphic resolution of this study in the northern Bighorn Basin.

We use the following criteria to identify various source lithologies. TSA3 includes the Upper Cretaceous strata of the Lance Formation, Meeteetse Formation, Mesaverde Formation, Frontier Formtation, Mowry Shale, and Muddy Sandstone deposited in the foredeep of the Sevier foreland basin. These formations are about 2 km thick, and covered the Laramide Ranges (McGookey et al., 1972). These units are dominated by marine shales and contain lesser amounts of fluviodeltaic and nearshore marine sandstone lithofacies. Erosion of these units would provide comparatively

fine-grained sediment to the basin, and sandstone compositions dominated by quartz and sedimentary lithic grains. The detrital zircon signature of the TSA3 strata is characterized by a significant proportion (>40%) of CCM zircons and to a lesser extent YM zircons (Fig. 8). Especially pronounced is an age peak at ~98 Ma found within all the constituent formations, and a comparatively minor peak at ~75 Ma found within the Lance and Mesaverde formations (May et al., 2013). TSA3 should be the first strata unroofed within the Laramide ranges surrounding the Bighorn Basin, and any rivers with that sediment sources exhibit a similar detrital zircon signature.

TSA2 includes Jurassic and Lower Cretaceous strata of the Greybull Sandstone, Cloverly Formation, Morrison Formation, and Sundance Formation originally deposited in the Sevier foreland basin system (DeCelles, 2004; May et al., 2013). These siliciclastic units tend to be more sand-rich than TSA3 strata and contain isolated intervals of conglomeratic units that contain chert and quartzite (e.g. Pryor Conglomerate of the Cloverly Formation). In total these units represent 200-400 m of stratigraphic thickness in the area. The expected sandstone composition of these strata is also quartz-rich with lithic sedimentary fragments. The detrital zircon U-Pb signature of TSA2 differs dramatically from that of TSA3. CCM zircons are comparatively rare, and display a range of peaks at 110, 159, 164, and 170 Ma (Fig. 8). There is an abundance of AOO grains and particularly abundant GP grains (Fig. 8). AOO peaks include a distinctive peak at both 421 and 594 Ma.

TSA1 encompasses the early Mesozoic and Paleozoic strata in the region: Chugwater Formation, Goose Egg/Phosphoria Formation, Tensleep Sandstone, Amsden Formation, Madison Limestone, Bighorn Dolomite, Gros Ventre Formation, and Flathead Sandstone deposited when the western margin of North America was a passive margin and during the Ancestral Rockies Orogeny. These units are overall coarser than TSA3 and contain carbonates capable of generating

conglomeratic debris. The typical thickness of these combined formations around the Bighorn Basin is ~1200 m. The detrital zircon U-Pb signature of TSA1 contains a distinct AOO peak at 422 Ma and sizeable GP and YM peaks (Fig. 8). Additionally, it contains a significant peak at ~2.7 Ga (Fig. 8). Finally, the gneissic and granitic basement in the Bighorn, Owl Creek, and Beartooth mountains displays ages ~2.8 and 3 Ga (Gast et al., 1958; Frost & Fanning 2006). This crystalline rock is rich in zircons and should produce a distinctive and dominant Archean peak that swamps out signatures from the comparatively zircon-poor, Phanerozoic sedimentary strata. Exposure of crystalline basement should also produce a higher proportion of feldspar and Lv in basin fluvial sandstones.

Sandstone composition and detrital zircon geochronologic data indicate the major provenance source was Cretaceous and Jurassic siliciclastic strata (TSA2 and TSA3) for the eastern and southeastern river systems. A recycled sedimentary source is consistent with the relatively quartz-rich sandstones whose lithic component is dominated by sedimentary rock fragments (Fig. 4; 5). Additionally, researchers have found reworked Cretaceous shark teeth and marine dinoflagellates within the Willwood Formation (Baczynski et al., 2013). In the eastern study area, the detrital zircon signature of the Willwood Formation shows large age peaks at ~92 and ~1780, and high percentages of zircons within the coastal Cordilleran magmatic arc and Yavapai-Mazatzal province age ranges (Table 2). This is similar to the zircon age spectra pattern of Upper Cretaceous fluviodeltaic strata and marine shales (Fig. 8). Taken as a whole the CCM range for these Upper Cretaceous strata is dominated by the ~98 Ma peak within the Upper Cretaceous strata, with a minor peak at ~75 Ma present in the Lance and Mesaverde Formations (May et al., 2013). The smaller contribution of ~75 Ma zircon grains is mimicked in the eastern and southeastern Willwood Formation zircon samples. However, the CCM percentage component in Cretaceous

strata dwarfs the other primary zircon sources, accounting for over 40% of the zircon ages in the respective formations (Fig.8; May et al., 2013). Although the percentage of grains falling in the CCM is high for the eastern Willwood Formation zircon samples they do not exceed 40% (Table 2). Thus, a purely uppermost Cretaceous source (TSA3 of May et al., 2013) for the Willwood Formation is not likely. Instead the Willwood Formation must also have included sizeable sediment contributions from the Middle and Lower Cretaceous and Jurassic siliciclastic strata, diluting the CCM contributions (TSA2; Fig. 8). These strata contain significant quantities of zircons ultimately derived from the Appalachian-Ouachita orogen and Grenville province, and minor Archean-aged grains. The detrital zircon records lack a distinct, dominant Archean peak that would indicate exposure of zircon-rich crystalline basement. The southeastern Willwood Formation shows an increase in the percentage of NLP and WHR grains relative to the eastern Willwood Formation sample. This potentially reflects the partial unroofing of TSA1 strata.

This provenance differs strikingly from that of the Powder River Basin to the east of the Bighorn Mountains and the Wind River Basin to the south of the Owl Creek Basin. In those basins, unroofing patterns are clear in sandstone petrography, conglomerate clast composition, and detrital zircon U-Pb signals. In the Powder River Basin there is an unroofing pattern within conglomeratic alluvial fan deposits and structural relationships that indicate the Precambrian basement was exposed by the early Eocene (Whipkey et al., 1991; Hoy and Ridgway, 1997). Indeed, the Wasatch Formation in the Powder River Basin (equivalent to the Willwood Formation) contains a detrital zircon U-Pb signal that is dominated by Archean ages consistent with derivation from the Bighorn Mountain basement (Anderson et al., 2019). Structural analysis of Hoy and Ridgway (1997) indicate ~10 kilometers structural relief by the Eocene and thermochronologic data suggest rapid exhumation starting ~71 Ma (Peyton et al., 2012). Overall

the provenance history observed is consistent with the east-vergent, moderately steep reverse fault providing the majority of topographic relief on the eastern flank of the Bighorn Mountain range, and the western flank remaining largely a gentle west-dipping homocline. The exception is the Five Spring thrust fault that verges to the west in the northwestern portion of the Bighorn Mountains (Wise & Obi, 1992; Narr, 1993). Crowley et al. (2002) identified anomalously low age-elevation correlations for (U-Th)/He apatite ages of basement rocks in the Five Springs area and suggested this could be due to extremely slow exhumation in the Cretaceous or a fossil, pre-Laramide He partial retention zone. They favored the later, however, our provenance record suggests comparatively little of the Phanerozoic cover had been removed by the Eocene along the western flank of the Bighorn Mountains. Very slow exhumation rates are possible. However, the extreme dominance of Archean ages in the Eocene Wasatch Formation in the Powder River Basin (Anderson et al., 2019) suggest faster exhumation on the eastern flanks, and could affect some of the complexity of the thermochronologic signals (Crowley et al., 2002). The Owl Creek Mountains do not have a comparative thermochronologic dataset, but provenance records of Fan et al. (2011) indicate a similar asymmetric erosion pattern on the southern and northern flanks of the mountains. Specifically, in the early Eocene, there are conglomeratic units that contain Paleozoic limestones and an increasing abundance of crystalline basement clasts up-section in the Wind River Basin (Fan et al., 2011). By post-dating U-Pb detrital zircon age spectra contain a large peak ~2.7 Ga (Fan et al., 2015)

Southwestern river deposits contain indicators of a more complex provenance. Fluvial sandstone composition from the Fort Union and Willwood formations show a very slight increase in the amount of volcanic lithic fragments as compared to the east and southeast samples, suggesting greater influence of an igneous source lithology. Detrital zircon signatures for the

southwest Fort Union and Willwood Formations both show the similar dominant age peaks and primary source areas. The major primary sources are the CCM with a dominant age peak around ~95 Ma and a minor peak at ~75 Ma, YM grains with a dominate age peak at ~1745 Ma and WHR peaks at around 2700 to 2780 Ma. This suggests TSA3 units were major contributors of sediment, but the southwestern Willwood Formation also shows increased AOO and GP grain percentages consistent with TSA2 source lithologies, and partial exposure of TSA3 source lithologies to obtain the WHR grains. Broadly, these are similar to age spectra in the southeastern and eastern portions of the Bighorn Basin (Fig. 5). Some of this sediment could have been derived from the Sevier fold-and-thrust belt to the southeast, but an additional source could be reworking and erosion of the Cody Arch, which was an area of tectonism during the Laramide (Steidtman & Middleton, 1991). Specifically, between the Wind River Range and Beartooth Range along the Cody Arch, various portions of the Phanerozoic stratigraphy are "missing" and presumably eroded. Most notably missing are the Mesozoic siliciclastic strata of TSA3 and TSA2. Only in some areas do Eocene-aged scours and paleo-valley cut into Paleozoic carbonate rocks (Malone et al., 2014b). Alternatively, another potential source, the Paris-Meade-Absaroka thrust system would have equivalent strata.

However, these TSA3 and TSA2 strata could not have been the only sediment source to this area of the basin. Quartzite-rich conglomeratic units interpreted as braided rivers are also present in the Fort Union and Willwood formations in the southwestern Bighorn Basin and have no local source within adjacent Laramide structures. Previous researchers have attributed the source to the hypothesized Targhee uplift (Love, 1973), from the Paris Willard-Putnam thrust sheet and reworking of Harebell and Pinyon conglomerates near Jackson Hole, Wyoming, (Schmitt & Steidtmann, 1990), transport through the Monida transverse zone (Lawton et al. 1994), and from

Eocene paleo-valleys east of the Idaho Batholith as potential sources (Ryder & Scholten, 1973; Janecke et al., 2000). More broadly, the provenance of these quartzite clasts could be from the Proterozoic Belt-Purcell Supergroup to the north in Montana and northeastern Idaho or the Brigham Group of southeastern Idaho. Malone et al. (2017) tested this hypothesis by characterizing the U-Pb detrital zircon signatures of clasts within the Pinyon and Harebell near the Wyoming Sevier fold-and-thrust belt as well as the Fort Union and Willwood Formations in the southwestern Bighorn Basin. A source dominated by quartzite input from the Belt-Purcell Group as proposed by Ryder and Schlten (1973) and Janecke et al. (2000) amongst others would contain a distinct and large ~1.4 Ga peak. However, Malone et al. (2017) found a diverse set of peaks with the majority of the grains falling within the YM province, but also anomalously young grains ~1.0 Ga more consistent with derivation from the lower Brigham Group of southeastern Idaho. Detrital gold found in the conglomerates also suggests that they were derived from the Harebell and Pinyon formations or a similar source (Antweiler and Love, 1967, Kraus, 1982). Importantly, this could also be a source for the slight increased volcanic sedimentary grains observed, as these Proterozoic strata also contain volcanic rocks. These data suggest the majority of quartzite-rich coarse clastics were derived from an interior ramp within the Sevier fold-and-thrust belt wherein the Paris sheet was uplifted by the active Absaroka thrust fault.

Sandstone compositions and detrital zircon geochronology in the northern region of the basin indicate a mixture of sediment sources for the Fort Union and Willwood formations that include significant input from crystalline basement. Specifically, there is a greater range of compositions that include greater feldspar abundance and volcanic lithic fragments, suggesting exposure and erosion of primary igneous material. Detrital zircon age spectra show all the age peaks seen in the east, southeast and southwest indicating erosion of TSA3 and TSA2 strata.

However, these northern strata also include carbonate clast-rich alluvial fan facies of the Beartooth Conglomerate, which has a much larger U-Pb zircon age peak at ~73 Ma than observed in other locations in the basin, and new peaks at ~2.45 and ~3.25 Ga. Moreover, the percentage of age determinations that fall within WHR (including ~2.7 Ga) is substantially higher than other areas in the basin (Table 2). The younger distinct age peak at ~73 Ma shows input of a new source, the Idaho Batholith, potentially the Boulder or Bitteroot lobe, but more likely the Tobacco Root lobe. The Bitterroot Lobe age is approximately 53 to 75 Ma, the Boulder Batholith is ~75 Ma, the Tobacco Root lobe is ~70 Ma (Foster & Fanning, 1979), whereas the Atlanta Lobe is around 68 to 98 Ma, with the majority of intrusion of ~98 Ma (Gaschnig et al. 2010). The age peaks around 2.45 and ~3.25 Ga, are relatively diagnostic as well and can be linked to crystalline basement of the Tobacco Root Mountains and Madison Range, respectively (Mogk et al., 1992; Krogh et al., 2011). An increase in the relative abundance of 2.7 Ga zircons suggests a basement source in the Beartooth Range (Mogk et al., 1992; Mueller et al., 1996), which is also reflected in the upper portions of the Beartooth Conglomerate clast composition (DeCelles et al., 1991). Thus, we propose a provenance for the northern Bighorn Basin that is a mixture of TSA3, TSA2, and TSA1 derived from both the more local Beartooth Conglomerate, but also a fluvial system that drains the Tobacco Root Mountains and Madison Range, including the Tobacco Root lobe of the Idaho Batholith and/or Boulder Batholith. This river system would have run along the southern margin of the Beartooth Range before entering the Bighorn Basin (Fig. 9).

Finally, in the north we examined the up-section changes in provenance. The age peaks seen at 2450 to 2550 Ma are absent in the Tiffanian 2-4 strata but present in the overlying strata. This suggests that most of the unroofing occurred early during the Bighorn Basin formation, and that the major shift in provenance occurred due to input from extra-basinal sources rather than

major changes in lithologies exposed in Laramide uplifts across the basin. These provenance records are consistent with recent thermochronologic work by Carrapa et al. (2019) that suggests cooling and exhumations within these Laramide structures much earlier in the Cretaceous. Presumably, a thick sedimentary sequence was breached in the Tobacco Root Mountains and Madison Range by Clarkforkian time.

The Crandall Conglomerate is interpreted to be a series of fluvial deposits that formed during Laramide deformation as the Beartooth Mountains uplifted to the northeast forming deep, narrow canyons (Pierce and Nelson, 1973). This conglomerate is composed of mostly carbonate material from the Mississippian Madison Limestone, Devonian Jefferson Formation, and Ordovician Bighorn Dolomite with lesser amounts of Cambrian and Precambrian material (Pierce, 1957). Provenance analysis for the Crandall Conglomerate by Malone et al. (2014) interprets that the conglomerate has sources from the basement rock exposed in the Beartooth uplift, the ancestral Targhee Uplift, and different lobes of the Idaho Batholith.

Provenance & Basin Stratigraphic Patterns

Several researchers have noted spatial variability in the character of early Paleogene deposition within the Bighorn Basin (Hickey, 1980; Bown, 1980a,b; Wing et al., 2005; Kraus, 1982; 1992; 2002; Kraus & Middleton, 1987; Kraus & Gwinn, 1997; Kraus & Riggins, 2007; Foreman, 2014; Owen et al., 2017). Here we will focus on comparing patterns across the basin. This includes the transition from the Fort Union Formation to the Willwood Formation, the alluvial response to the PETM, and the variation in sand body characteristics and prevalence geographically across the basin.

As noted previously, the transition between the Fort Union and Willwood Formations is time transgressive across the Bighorn Basin. In most places the lithostratigraphic transition occurs with the Paleocene-Eocene boundary marked by the negative carbon isotope excursion of the PETM (Rose, 1981; Koch et al., 1992; Wing et al., 2000; Wing et al., 2005; Kraus & Riggins, 2007; Foreman, 2014). However, in the northern basin, the lithologic transition preceded the P-E boundary, perhaps by as much as 1 million years (Bown, 1981; Wing et al., 2000; Secord et al., 2006). Thus, the control of the lithogic change changes between the Fort Union and Willwood formations was related to a long-term, persistent boundary condition change rather than the transient PETM.

Kraus and Riggins (2007) note floodplain strata in the northern basin are coarser than south and southeastern floodplain strata and suggest the difference in drainage conditions correspond with a coarser grain size distribution in overbank strata in the northern basin (Kraus & Riggins. 2007), presumably transferred from the northern, axial river systems carrying coarser sediment loads themselves as compared to eastern and southern transverse rivers. This observation fits with our provenance analysis since the western sediment sources eroded more resistant lithologies to the Bighorn Basin river systems as compared to the eastern transverse rivers. Moreover, the input of sediment from the crystalline Tobacco Root Mountain and Madison Range roughly corresponds with the formational contact and might have sufficiently coarsened the overbank for the shift to occur. This is also consistent with the greater supply of sand-sized sediment from western sources as reflected in the prevalence and larger size of fluvial sand bodies in the western basin compared to the eastern and southern basins (Owen et al., 2017). Alternatively, this change could be related to reduction in subsidence rates within the basin. Clyde et al. (2007) provide a subsidence history for the basin that shows a slight reduction in rates roughly corresponding with the P-E boundary.

Assuming sediment supply remained constant, this would cause progradation of the alluvial system and displace the "under-filled" basin condition of the Fort Union Formation. Evidence for this can be found in the replacement of paludal and lacustrine Fort Union strata in southern Montana portion of the Bighorn Basin with Willwood Formation fluvial sand bodies and red bed overbank strata.

An anomalously thick and laterally extensive multi-story amalgamated fluvial sand body crops out in the northern Bighorn Basin within the PETM stratigraphic interval and has been interpreted to indicate greater channel mobility (Foreman, 2014; Kraus et al., 2015). Our provenance analysis of this sandstone shows no major shift in source area spanning this Boundary Sandstone, further supporting a climate-driven hypothesis of the formation of this sandstone. Moreover, our provenance analysis implies one of the reasons no equivalent Boundary Sandstone has been found in the southern or eastern Bighorn Basin is related to the grain size distribution of the source lithologies within the Bighorn Mountains. If the vast majority of exposed strata were clay- and silt-rich uppermost Cretaceous strata then there may have simply been insufficient sand-sized sediment available to generate a substantial sand body.

The recent study by Owen et al. (2017) on sand body geometries and their internal architecture across the Bighorn Basin provides the best combination of quantitative and broad synthesis of depositional patterns that currently exists. They document the relative proportions of isolated, amalgamated, semi-amalgamated, and massive sand bodies across much of the basin, grouping the Fort Union and Willwood Formations together. They find the southwestern and northwestern margins dominated by conglomeratic massive sand bodies, interpreted as braided fluvial units, and alluvial fan units, respectively. This assessment is consistent with previous studies (Kraus, 1982; DeCelles et al., 1991) and also by the absence of similarly coarse units within

the basins geographic center, southern margin, and eastern margin (Owen et al., 2017). Amalgamated and semi-amalgamated sand bodies, representing persistent areas of meandering river occupation, are more common along the west central and northern portions of the basin (Owen et al., 2017). These are the hypothesized axial river systems that drained northward by previous studies (Kraus & Middleton, 1987; Kraus, 2001), and as the medial portions of a distributive fluvial system by Owen et al. (2017). Isolated, lenticular sand bodies dominate along the east central, eastern, and southeastern margins of the basin along with cut-and-fill structures (Bown et al., 1994; Wing et al., 2005; Owen et al., 2017). These are interpreted as solitary meandering river deposits, interpreted as transverse rivers by previous studies (Kraus & Middleton, 1987; Kraus, 2001) and the distal portions of a distributive fluvial system by Owen et al. (2017). The distributive fluvial system proposed by Owen et al. (2017) invokes downstream fining via selective deposition of coarse sediment sizes and abrasion as well as bifurcation of more proximal channels into smaller and smaller channels to produce the spatial changes in sand body prevalence and grain size. We agree with their model for the majority of the western and central portions of the basin but suggest the mudrock-dominated eastern and southern portions of the basin and smaller, isolated fluvial sand bodies are more likely a consequence of the finer grain size distribution provided from Bighorn Mountain and Owl Creek Mountain catchments. Interestingly, Hoy & Ridgway (1997) invoke a provenance control on the vertical stratigraphic evolution of the Powder River Basin. They suggest the initial deposition of Paleocene Lebo Shale lacustrine interval was largely driven by erosion of TSA3 and TSA2 strata, and later Paleocene alluvial fan deposits of the Tongue River Member of the Paleocene are only possible when carbonates of TSA1 are exposed. The stratigraphic evolution is completed when the composition of the allluvial fans shifts to one rich in crystalline basement in the Eocene Moncrief Formation.

CONCLUSIONS

In this paper we assessed the provenance of the early Paleogene strata in the Bighorn Basin using a combination of new and compiled data including paleocurrent measurements, sandstone petrographic composition, and detrital-zircon U-Pb geochronology. We found a broad similarity in the provenance of the Fort Union and Willwood formations across the basin. However, their provenance signatures vary spatially, providing insights in the tectonic and stratigraphic evolution of the basin.

Paleocurrents show a pattern consistent with a system of transverse rivers draining towards the basin center. These transverse rivers contributed sediment loads to an axial system that flowed northwards into southern Montana between the Beartooth and Pryor Mountains. These data are consistent with previous research that show that during the Paleocene through Eocene, the Bighorn, Owl Creek and Beartooth Mountains were all topographic highs and supplying sediment to the basin. Additionally, paleocurrents suggest transport of sediment over the Cody Arch in the southwestern portion of the basin throughout most of the Paleocene and early Eocene.

Detrital zircon age spectra and sandstone petrography show no difference in provenance between the Fort Union and Willwood Formations in the basin, but the lithologies eroded in the hinterland catchments differ spatially. Catchments in the Bighorn Mountains and the Owl Creek Mountains had unroofed Upper Cretaceous shales and fluviodeltaic strata and likely minor amounts of lower Mesozoic and uppermost Paleozoic siliciclastic units. This contrasts with provenance records in the Powder River and Wind River basins adjacent to the eastern and southern sides of the Bighorn and Owl Creek Mountains, respectively, which contain evidence for Precambrian crystalline provenance (Hoy & Ridgway, 1997; Fan et al., 2011; Anderson et al.,

2019). We view this as a consequence of the structural geometry from the drape folds over the eastern and southern verging basement thrusts in the Bighorn and Owl Creek mountains. Major atmospheric moisture transport directions and rainfall patterns may have exacerbated asymmetric unroofing with preferential rainout on mountains more proximal to the paleo-Gulf of Mexico moisture source (Sewall & Sloan, 2006). This difference in source lithology led to fine-grained fluvial and overbank strata in the eastern and southeastern Bighorn Basin and synorogenic, conglomeratic alluvial fans in the Powder River and Wind River basins.

The Fort Union and Willwood Formations in the southwestern basin show input consistent with mixed provenance from the Sever Thrust Belt (both Wyoming and Helena Salients). This likely also included erosion of portions of the Cody Arch removing much of the Mesozoic and portions of the Paleozoic sedimentary cover (Malone et al., 2017; 2017). We attribute the ability of Sevier hinterland sediment to be exported out of the fold-and-thrust belt via the Monida transverse structural zone proposed by Lawton et al. (1994). We propose the larger catchment size and exposure of quartzites, cherts, and igneous/metamorphic basement rocks led to deposition of coarse-grained lithofacies being dominant within the southwestern Bighorn Basin. The northern Bighorn Basin samples show a more mixed sediment provenance consistent with derivation from Phanerozoic cover, Sevier fold-and-thrust belt, and Precambrian basement from the Beartooth, Tobacco Root, and Madison ranges as well as the Idaho Batholith. This mixture is consistent with this area being dominated by an axial river system. Sediment input from the Beartooth Conglomerate alluvial fan systems transitioned into this northward draining river system over a relatively short distance.

The lack of major provenance and paleodrainage directions changes between the formations suggests that the transition from Fort Union to Willwood formations within the Bighorn Basin is

likely due to a combination of tectonic and climatic shifts. The changes were likely due to a reduction in subsidence perhaps due to regional quiescence of the Laramide Orogeny, greater provision of basement-derived coarse sediment loads, and an increase in the seasonality or climatic variability of rainfall as carbon dioxide levels and temperatures rose towards the Early Eocene Climatic Optimum.

WORKS CITED

Adams, J., Kraus, M., Wing, S., 2011, Evaluating the use of weathering indices for determining mean annual precipitation in the ancient stratigraphic record: Palaeogeography Palaeoclimatology Palaeoecology, v. 309, p. 358 – 366, doi: 10.1016/j.palaeo. 2011.07.004.

Anderson, I., Malone, D.H., and Craddock, J.P., 2019, Preliminary detrital zircon U-Pb geochronology of the Wasatch Formation, Powder River Basin, Wyoming: The Mountain Geologist, v. 56, p. 247-265,

Ayers, W. B., 1986, Lacustrine and fluvial-deltaic depositional systems, Fort Union Formation (Paleocene), Powder River Basin, Wyoming and Montana: AAPG Bulletin, v. 70, n. 11, p. 1651–1673.

Baczynski, A.A., McInerney, F.A., Wing, S.L., Kraus, M.J., Bloch, J.I., Boyer, D.M., Secord, R., Morse, P.E., and Fricke, H.C., 2013, Chemostratigraphic implications of spatial variation in the Paleocene-Eocene thermal maximum carbon isotope excursion, SE Bighorn Basin, Wyoming: Geochemistry Geophysics Geosystems, v. 14, p. 4133–4152,

Bown, T.M., 1980a, Summary of Latest Cretaceous and Cenozoic Sedimentary, Tectonic, and Erosional Events, Bighorn Basin, Wyoming. in P.D. Gingerich eds., Early Cenozoic

Paleontology and Stratigraphy of the Bighorn Basin, Wyoming, Papers on Paleontology No. 24, Museum of Paleontology The University of Michigan, p. 25-32.

Bown, T.M., 1980b, The Willwood Formation (Lower Eocene) of the southern Bighorn Basin, Wyoming and its Mammalian Fauna. in P.D. Gingerich eds., Early Cenozoic Paleontology and Stratigraphy of the Bighorn Basin, Wyoming, Papers on Paleontology No. 24, Museum of Paleontology The University of Michigan, p. 127-138.

Bown T.M. and M.J. Kraus, 1981. Lower Eocene alluvial paleosols (Willwood Formation, northwest Wyoming, U.S.A.) and their significance for paleoecology, paleoclimatology, and basin analysis. *Palaeogeography, Palaeoclimatology, Palaeoecology v.* 34, p. 1-30.

Bown, T.M., ,Rose, K.D., Simons, E.L., and Wing, S.L., 1994, Distribution and stratigraphic correlation of Upper Paleocene and Lower Eocene fossil mammal and plant localities of the Fort Union, Willwood, and Tatman Formations, southern Bighorn Basin, Wyoming. US Geological Survey professional paper 1540, p. 1-103.

Bowen, G. J., Bralower, T. J., Delaney, M. L., Dickens, G. R., Kelly, D. C., et al., 2006, Eocene hypothermal event offers insight into greenhouse warming: Eos, v. 87, no. 17, p. 165–169.

Burchfiel, B.C., and Davis, G.A., 1975, Nature and controls of Cordilleran orogenesis in the western United States: Extensions of an earlier synthesis: American Journal of Science, v. 275A, p. 363–396.

Craddock, J.P., Malone, D.H., Porter, R., MacNamee, A., Mathisen, M., Kravitz, K. and Leonard, A., 2015. Structure, Timing, and Kinematics of the Early Eocene South Fork Slide, Northwest Wyoming, USA. The Journal of Geology, v. 123(4), p.311-335.

Carrapa, B., DeCelles, P.G., Romero, M.C., 2019, Early inception of the Laramide Orogeny in

southwestern Montana and northern Wyoming: Journal of Geophysical Research, v. 124, p. 2102-2123.

Chetel, L.M., Janecke, S.U., Carroll, A.R., Beard, B.L., Johnson, C.M. and Singer, B.S., 2011, Paleogeographic reconstruction of the Eocene Idaho River, North American Cordillera: Geological Society of America Bulletin, v. 123, p. 71-88. https://doi.org/10.1130/B30213.1

Clyde, W., Hamzi, W., Finarelli, J., Wing, S., Shankler, D., Chew, A., 2007, A basin-wide magnetostratigraphic framework for the Bighorn Basin, WY: Geological Society of America Bulletin, v. 119, p, 848-859, doi.10.1130/B26104.1.

Clyde, W.C. & Gingerich, P.D., 1998, Mammalian community response to the latest Paleocene thermal maximum: an isotaphonomic study in the northern Bighorn Basin,Wyoming: Geology, v. 26, p. 1011–1014.

Crowley, R. D., Reiners, P. W., Reuter, J. M., & Kaye, G. D., 2002, Laramide exhumation of the Bighorn Mountains, Wyoming: An apatite (U-Th)/He thermochronology study: Geology, v. 30, p. 27–30.

D'Ambrosia, A., Clyde, W., Fricke, H., Gingerich, P., Abels, H., 2017, Repetitive mammalian dwarfing during ancient greenhouse warming events: Science Advances 3. e1601430. Doi. 10.1126/sciadv.1601430.

Davis, S.J., Mix, H.T., Wiegand, B.A., Carroll, A.R., And Chamberlain, C.P., 2009, Synorogenic evolution of large-scale drainage patterns: isotope paleohydrology of sequential Laramide basins: American Journal of Science, v. 309, p. 549–602.

Davis, S.J., Dickinson, W.R., Gehrels, G.E., Spencer, J.E., Lawton, T.F., And Carroll, A.R., 2010, The Paleogene California River: evidence of Mojave–Uinta paleodrainage

from U-Pb ages of detrital zircons: Geology, v. 38, p. 931–934.

Dickinson, W. R., and Gehrels, G. E., 2003, U-Pb ages of detrital zircons from Permian and Jurassic eolian sandstones of the Colorado Plateau, USA: Paleogeographic implications, Sediment. Geol., v. 163(1–2), p. 29–66, doi:10.1016/S0037-0738(03)00158-1.

DeCelles, P.G., 2004, Late Jurassic to Eocene evolution of the Cordilleran thrust belt and foreland basin system, western U.S.A.: American Journal of Science, v. 304, p. 105–168, doi:10.2475/ajs.304.2.105.

Dickinson, W. R., and Gehrels G. E., 2008, Sediment delivery to the Cordilleran foreland basin: Insights from U-Pb ages of detrital zircons in Upper Jurassic and Cretaceous strata of the Colorado Plateau: American Journal of Science, v. 308(10), p. 1041–1082, doi:10.2475/01.2008.01.

Dickinson, W.R., Klute, M.A., Hayes, M.J., Janecke, S.U., Lundin, E.R., Mckittrick, M.A. & Olivares, M.D., 1988, Paleogeographic and paleotectonic setting of Laramide sedimentary basins in the central Rocky Mountain region: Geological Society of America Bulletin, v. 100, p. 1023–1039.

Dickinson, J.A., Cook, S.D. and Leinhardt, T.M., 1985, The measurement of shock waves following heel strike while running: Journal of Biomechanics, v.18, p. 415-422.

Dickinson, W.R., Beard, S., Brakenbridge, F., Erjavec, J., Ferguson, R., Inman, K., Knepp, R., Lindberg, P., Ryberg, P., 1983, Provenance of North American Phanerozoic sandstones in relation to tectonic setting: Geological Society of America Bulletin v. 94, p. 222–235.

Dickinson, W.R., and Snyder, W.S., 1978, Plate tectonics of the Laramide orogeny, in Matthews, W., III, ed., Laramide Folding Associated with Basement Block Faulting in the Western United States: Geological Society of America Memoir, v.151, p. 355–366.,

https://doi .org/10.1130/MEM151-p355.

Dickinson, W.R., 1970, Interpreting detrital modes of graywacke and arkose: Journal of Sedimentary Petrology, v. 40, p. 695–707.

Duller, R.A., Whittaker, A.C., Fedele, J.J., Whitchurch, A.L., Springett, J., Smithells, R., Fordyce, S., Allen, P.A., 2010, From grain size to tectonics: Journal of Geophysical Sciences: Earth Surface Processes 115, F03022.

Edmonds, D.A., Slingerland, R.L., 2011, Significant effect of sediment cohesion on delta morphology: Nature Geoscience, v. 3, p. 105-109.

Feeley T C and Cosca M A 2003 Time vs. composition trends of magmatism at Sunlight volcano, Absaroka volcanic province, Wyoming; Geol. Soc. Am. Bull. V. 115 p. 714–772,

Folk, R.L., 1980, Petrology of Sedimentary Rocks: Hemphill Publishing, Austin, TX, 184p.

Foreman, B.Z., 2014, Climate-driven generation of a fluvial sheet sand body at the Paleocene Eocene boundary in north-west Wyoming (USA): Basin Research, v. 26, p. 225–241.

Foreman, B.Z., Heller, P.L., Clementz, M.T., 2012, Fluvial response to abrupt global warming at the Paleocene/Eocene boundary: Nature, v. 491, p. 92-95.

Foster, D.A.; Fanning, C.M., 1997, Geochronology of the northern Idaho Batholith and the Bitterroot metamorphic core complex: magmatism preceding and contemporaneous with extension: Geological Society of America Bulletin, v. 109, p. 379–394.

Fricke, H.C., Clyde, W.C., O'neil, J.R., Gingerich, P.D., 1998, Evidence for rapid climate change in North America during the latest Paleocene thermal maximum: oxygen isotope compositions of biogenic phosphate from the Bighorn Basin (Wyoming): Earth Planet. Sci. Lett., v. 160, p. 193–208.

Frost, C.D., and Fanning, M., 2006, Archean geochronological framework of the Bighorn Mountains, Wyoming: Canadian Journal of Earth Sciences, v. 43, p. 1399- 1418, doi:10.1139/e06-051.

Gast, P.W., Kulp, J.L., L, Leon., 1958, Absolute age of Early Precambrian rocks in the Bighorn Basin of Wyoming and Montana, Am. Geophys. Union. Trans., v. 39, p. 322 - 334, doi. 10.1029/TR039i002p00322.

Gaschnig, R.M.; Vervoort, J.D.; Lewis, R.S.; McClelland, W.C., 2010, Migration magmatism in the northern US Cordillera: in situ U-Pb geochronology of the Idaho batholith: Contributions to Minerology and Petrology, v. 159, p. 863-883.

Gehrels, G., Valencia, V. & Pullen, A. 2006. Detrital zircon geochronology by laser-ablation multicollector ICPMS at the Arizona LaserChron Center. The Paleontological Society Papers, 12, 67–76.

Gehrels, G.E., Valencia, V.A. & Ruiz, J. 2008. Enhanced precision, accuracy, efficiency, and spatial resolution of U–Pb ages by laser ablation-multicollector-inductively coupled plasma-mass spectrometry. Geochemistry, Geophysics, Geosystems, 9, Q03017, https://doi.org/ 10.1029/2007GC001805

Gehrels, G., 2014, Detrital Zircon U-Pb Geochronology Applied to Tectonics: Annual Review of Earth and Planetary Sciences, v. 42, p. 127-149, doi.10.1146/annurev-earth-050212-124012.

Gehrels, G., & Pecha, M., 2014, Detrital zircon U-Pb geochronology and Hf isotope geochemistry of Paleozoic and Triassic passive margin strata of western North America: *Geosphere*, v. *10*(1), p. 49-65. DOI: 10.1130/GES00889.1

Gehrels, G. E., R. Blakey, K. E. Karlstrom, J. M. Timmons, B. Dickinson, and M. Pecha, 2011,

Detrital zircon U-Pb geochronology of Paleozoic strata in the Grand Canyon, Arizona: Lithosphere, v. 3, p. 183–200, doi:10.1130/L121.1.

Gao, Min, and Majie Fan., 2018, Depositional Environment, Sediment Provenance and Oxygen Isotope Paleoaltimetry of the Early Paleogene Greater Green River Basin, Southwestern Wyoming, U.S.A.: *American Journal of Science*, vol. 318, no. 10, p. 1018–1055., doi:10.2475/10.2018.02.

Gingerich, P. D., 2003, Mammalian Responses to Climate Change at the Paleocene-Eocene Boundary: Polecat Bench Record in the Northern Bighorn Basin, Wyoming: Special Paper of the Geological Society of America. v. 369, p. 463-478, doi.10.1130/0-8137-2369-8.463.

Gingerich, P. D., 2001, Biostratigraphy of the continental Paleocene-Eocene boundary interval on Polecat Bench in the northern Bighorn Basin. In: Gingerich, P. D. (Ed.), Paleocene-Eocene Stratigraphy and Biotic Change in the Bighorn and Clarks Fork Basins, Wyoming, University of Michigan Papers on Paleontology, v. 33, p. 37-71.

Gingerich, P. D., 1992, Marine Mammals (Cetacea and Sirenia) from the Eocene of Gebel Mokattam and Fayum, Egypt: Stratigraphy, Age and Paleoenvironments. The University of Michigan Museum of Paleontology Papers on Paleontology. v. 30, p. 1-84.

Gingerich, P. D., 1989, New Earliest Wasatchian Mammalian Fauna from the Eocene of Northwestern Wyoming: Composition and Diversity in a Rarely Sampled High-Floodplain Assemblage: Univ. Mich. Pap. Paleontology, v. 28, p. 1-97.

Gingerich, P. D., 1980, Early Cenozoic paleontology and stratigraphy of the Bighorn Basin, Wyoming. Univ. Mich. Pap. Paleontology, v. 24, p. 1-46.

Gingerich, P. D. and W.C. Clyde. 2001, Overview of mammalian biostratigraphy in the Paleocene- Eocene Fort Union and Willwood formations of the Bighorn and Clarks Fork basins. In P. D. Gingerich (ed.), Paleocene-Eocene stratigraphy and biotic change in the Bighorn and Clarks Fork basins, Wyoming, University of Michigan Papers on Paleontology, v. 33, p. 1-14.

Gunnell GF. 1989, Evolutionary history of Microsyopoidea (Mammalia, ?Primates) and the relationship between Plesiadapiformes and Primates Univ. Mich. Pap. Paleontol. v. 27, p.1–157

Hagen, E.S., Shuster, M.W. & Furlong, K.P., 1985, Tectonic loading and subsidence of intermontane basins, Wyoming foreland province: Geology, v. 13, p. 585–588.

Hickey, L.J., 1980, Paleocene stratigraphy and flora of the Clark's Fork Basin. p. 33-49 in: Early Cenozoic Paleontology and Stratigraphy of the Bighorn Basin, Wyoming 1880–1980 (Ed by P.D. Gingerich) Univ. Michigan Pap. Paleontol., v. 24.

Ingersoll, R.V, Bullard, T.F., Ford, R.L., Grimm, J.P., Pickle, J.D., And Sares, S.W., 1984, The effect of grain size on detrital modes: a test of the Gazzi–Dickinson point-counting method: Journal of Sedimentary Petrology, v. 54, p. 103–116, doi: 10.2475/ ajs.286.10.737.

Jackson, W.T., McKay, M.P., Bartholomew, M.J., Allison, D.T., Spurgeon, D.L., Shaulis, B., VanTongeren, J.A., and Setera, J.B., 2019, Initial Laramide tectonism recorded by Upper Cretaceous paleoseismites in the northern Bighorn Basin, USA: Field indicators of an applied end load stress: Geology, v. 47, p. 1059-1063.

Kennett, J.P. & Stott, L.D., 1991, Abrupt deep-sea warming, palaeoceanographic changes and benthic extinctions at the end of the Palaeocene: Nature, v. 353, p. 225–229

Kesling, R. V., & Chilman, R.B., 1987, *Dimorphic Middle Devonian paleocopan Ostracoda of the Great Lakes region.* Ann Arbor, Mich.: Museum of Paleontology, University of Michigan.

Koch, P.L., Zachos, J.C. & Gingerich, P.D., 1992, Correlation between isotope records in marine and continental carbon reservoirs near the Paleocene/Eocene boundary: Nature, v. 358, p. 319–322.

Kraus, M.J., 1982, Genesis of Early Tertiary Exotic Metaquartzite Conglomerates in the Absaroka-Bighorn Region, Northwest Wyoming: Wyoming Geological Association Guidebook, 33rd Annual Field Conference, p. 103-110

Kraus M.J., 1992, Alluvial response to differential subsidence: Sedimentological analysis aided by remote sensing, Willwood Formation (Eocene), Bighorn Basin Wyoming, USA. Sedimentology v. 39, p. 455-470.

Kraus, M.J. & Woody, D.T., Smith, J.J., & Dukic, V., 2015, Alluvial response to the Paleocene –Eocene Thermal Maximum climatic event, Polecat Bench, Wyoming (U.S.A.): Palaeogeography, Palaeoclimatology, Palaeoecology. 435. 10.1016/j.palaeo.2015.06.021.

Kraus, M.J., McInerney, F.A., Wing, S.L., Secord, R., Baczynski, A.A., and Bloch, J.I., 2013, Paleohydrologic response to continental warming during the Paleocene-Eocene thermal maximum, Bighorn Basin, Wyoming: Palaeogeography, Palaeoecology, Palaeoclimatology, v. 370, p. 196-208.

Kraus, M.J. & Riggins, S., 2007, Transient drying during the Paleocene-Eocene Thermal Maximum (PETM): analysis of paleosols in the Bighorn Basin, Wyoming: Palaeogeography, Palaeoecology, Palaeoclimatology, v. 245, p. 444–461.

Kraus, M.J., (1996). Avulsion deposits in lower Eocene alluvial rocks, Bighorn Basin,

Wyoming: Journal of Sedimentary Research, v. 66, p. 354-363.

Kraus, M.J., Aslan, A., 1993, Eocene hydromorphic paleosols: Significance for interpreting ancient floodplain processes: Journal of Sedimentary Petrology, v. 63, p. 453-463.

Kraus, M. J., 1992, Alluvial response to differential subsidence: sedimentological analysis aided by remote sensing, Willwood Formation (Eocene), Bighorn Basin, Wyoming, USA: Sedimentology, v. 39, p. 455-470. doi:10.1111/j.1365-3091.1992.tb02127.x

Kraus, M.J. & Middleton, L.T., 1987, Contrasting architecture of two alluvial suites in different structural settings. In: Recent Developments in Fluvial Sedimentology (Ed. By F.G. Ethridge) Soc. Econ. Paleo. Mineral. Spec. Pub., v. 30, p. 253–262.

Kraus, M.J., 1980, Genesis of a fluvial sheet sandstone, Willwood Formation Northwest Wyoming. In Gingerich, P.D., ed., Early Cenozoic paleontology and stratigraphy of the Bighorn Basin, Wyoming: University of Michigan Papers on Paleontology, v. 24, p.94-101.

Kraus, M.J., 1996. Avulsion deposits in lower Eocene alluvial rocks, Bighorn Basin, Wyoming: Journal of Sedimentary Research. v. 66, p. 354–363.

Kraus, M.J., 1997. Lower Eocene alluvial Paleosols: pedogenic development, stratigraphic relationships, and Paleosol/landscape associations: Palaeogeogr. Palaeoclimatol. Palaeoecol. v. 129, p. 387–406.

Kraus, M.J., 2002. Basin-scale changes in floodplain paleosols: implications for interpreting alluvial architecture: Journal of Sedimentary Research. v. 72, p. 500–509.

Kraus, M.J., Aslan, A., 1993. Eocene hydromorphic paleosols: significance for interpreting ancient floodplain processes: J. Sediment. Petrol. v. 63, p. 453–463.

Kraus, M.J., Aslan, A., 1999. Paleosol sequences in floodplain environments: a hierarchical

approach. In: Thiry, M., Simon-Coincon (Eds.), Palaeoweathering, Palaeosurfaces and Related Continental Deposits 27: IAS Special Publications, p. 303–321.

Kraus, M.J., Gwinn, B., 1997. Facies and facies architecture of Paleogene floodplain deposits, Willwood Formation, Bighorn Basin, Wyoming, USA: Sediment. Geol. v. 114, p. 33–54.

Kraus, M.J., Hasiotis, S.T., 2006. Significance of differentmodes of rhizolith preservation to interpreting paleoenvironmental and paleohydrologic settings: examples from Paleogen paleosols, Bighorn Basin, Wyoming, U.S.A: Journal of Sedimentary Research v. 76, p. 633–646. http://dx.doi.org/10.2110/jsr.2006.052.

Kraus, M.J., Middleton, L.T., 1987. Contrasting alluvial architecture of two Cenozoic sequences in different structural settings. In: Ethridge, F.G., Flores, M., Harvey, M.D. (Eds.), Recent Developments in Fluvial Sedimentology: SEPM Special Publication v. 39, p. 253–262.

Krogh, T.E., Kamo, S.L., Hanley, T.B., Hess, D.R., Dahl, P.S., and Johnson, R.E. 2011, Geochronology and gochemistry of Precambrian gneisses, metabasites, and pegmatite from the Tobacco Root Mountains, northwestern Wyoming craton, Montana: Canadian Journal of Earth Sciences, v. 48, p. 161-187.

Lawton, T.F., 2008, Laramide sedimentary basins, in Miall, A.D., ed., Sedimentary Basins of the World, v. 5, p. 429–450

Lawton, T.F., Boyer, S.E., and Schmitt, J.G., 1994, Influence of inherited taper on structural variability and conglomerate distribution, Cordilleran fold and thrust belt, western United States: Geology, v. 22, p. 339-42.

Love, J.D., 1973, Harebell Formation (Upper Cretaceous) and Pinyon Conglomerate (uppermost

Cretaceous and Paleocene), northwestern Wyoming: U.S. Geological Survey Professional Paper 734-A, 54 p.

Luo, Z. and P. D. Gingerich., 1999, Terrestrial Mesonychia to aquatic Cetacea: transformation of the basicranium and evolution of the hearing in whales. University of Michigan Papers on Paleontology, v. 31, p. 1-98.

Malone, D.H., Strow, M.L., and Craddock, J.P., 2012, Detrital zircon geochronology of the Willwood Formation in the Bighorn Basin, WY: implications for Eocene paleogeography: Geological Society of America Abstracts with Programs, v. 44, n. 7, p. 34.

Malone, D.H., Craddock, J.P., Link, P.K., Foreman, B.Z., Scroggins, M.A., and Rappe, J., 2017b. Detrital zircon geochronology of quartzite clasts, northwest Wyoming: Implications for Cordilleran Neoproterozoic stratigraphy and depositional patterns. Precambrian Research, v. 289, p. 115-128.

Malone, D.H., Craddock, J.P., and Mathesin, M.K.,2014a, Age and Provenance of Allochthonous VolcanicRocks at Squaw Peaks, WY: Implications for the Heart Mountain Slide: Mountain Geologist, v. 51, p. 321-336.

Malone, D.H., Breeden, J.R., Craddock, J.P., Anders, M.H., and #Macnamee, A.F., 2014b, Age and Provenance of the Eocene Crandall Conglomerate: Implications for Heart Mountain Faulting: Mountain Geologist, v. 51, p. 249-278.

Malone, D.H., Craddock, J.P., Tranel, L.R., and Mustain, M.R., 2014c, Age and Provenance of Eocene Volcanic Rocks and Hominy Peak, Northern Teton Range, WY: Implications for the Emplacement of the Heart Mountain Slide: Mountain Geologist, v. 51, p. 295-320.

Malone, D.H., Craddock, J.P., and Schroeder, K.A., 2014d, Detrital Zircon Age and Provenance

of Wapiti Formation (Eocene) Tuffaceous Sandstones, South Fork Shoshone River Valley, Wyoming: Mountain Geologist, v. 51, p. 279-294.

Malone, D.H., Craddock, J.P. Welch, J.L., and Foreman, B.Z., 2017a, Detrital Zircon U-Pb Geochronology and Provenance of the Eocene Willwood Formation, Northern Absaroka Basin, Wyoming: Mountain Geologist, v. 54,

Malone, D.H., Craddock, J.P., Link, P.K., Foreman, B.Z., Scroggins, M.A. and Rappe, J., 2017. Detrital zircon geochronology of quartzite clasts, northwest Wyoming: Implications for Cordilleran Neoproterozoic stratigraphy and depositional patterns. *Precambrian Research*, v. *289*, p.116-128.

May, S.R., Gray, G.G., Summa, L.L., Stewart, N.R., Gehrels, G.E.,. Pecha, M.E., 2013, Detrital zircon geochronology from the Bighorn Basin, Wyoming, USA: Implications for tectonostratigraphic evolution and paleogeography: Geological Society of America Bulletin, v. 125, p. 1403–1422, https://doi .org/10.1130/B30824.1.

McGookey, D.P., Haun, J.D., Hale, L.A., Goodell, H.G., McCubbin, D.G., Weimer, R.J., Wulf, G.R., 1972. Cretaceous System. In: Mallory, W.W. (Ed.), Geologic Atlas of the Rocky Mountain Region: Rocky Mountain Association of Geologists, Denver, p. 190–228.

McInernery, F.A. & Wing, S.L., 2011, The Paleocene-Eocene thermal maximum: a perturbation of carbon cycle, climate, and biosphere with implications for the future: Annu. Rev.Earth Planet. Sci., v. 39, p. 489–516.

Mogk, D. W., Mueller, P.A., and Wooden, J. L., 1992, The nature of Archean terrane boundaries: an example from the northern Wyoming Province: Precambrian Research, v. 55, p. 155-168.

Mueller, P.A., Wooden, J.L., Mogk, D.W., Nutman, A.P., Williams, I.S., 1996, Extended history of a 3.5 Ga trondhjemitic gneiss, Wyoming province, USA: Evidence from U-Pb systematics in zircon: Precambrian Research, v. 78, p 41-52.

Murphy, B.H., Farley, K.A. & Zachos, J.C., 2010, An extraterrestrial 3He-based timescale for the Paleocene-Eocene Thermal Maximum (PETM) from Walvis Ridge, IODP Site 1266. *Geochimica et Cosmochimica Acta*, v. *74*(17), p. 5098–5108.

Narr, W., 1993, Deformation of basement in basement-involved compressive structures, in Schmidt, C.J., et al., eds., Laramide basement deformation in the Rocky Mountain foreland of the western United States: Geological Society of America Special Paper 280, p. 107–123.

Neasham, J.W., Vondra, C.F., 1972, Stratigraphy and Petrology of the Lower Eocene Willwood Formation, Bighorn Basin, Wyoming: *GSA Bulletin*, v. 83, p. 2167–2180

Omar, G.I., Lutz, T.M. & Giegengack, R., 1994, Apatite fission- track evidence for Laramide and post-Laramide uplift and anomalous thermal regime at the Beartooth overthrust, Montana-Wyoming: GSA Bull., v. 106, p. 74–85.

Owen, A., Ebinghaus, A., Hartley, A.J., Santos, M.G.M. and Weissmann, G.S. 2017. Multi-scale classification of fluvial architecture: an example from the Palaeocene–Eocene Bighorn Basin, Wyoming. Sedimentology, 64, 1572–1596

Pagani, M., Caldeira, K., Archer, D., and Zachos, J.C., 2006, An Ancient Carbon Mystery: Science, v. 314, p. 1556–1557, doi: 10.1126/science.1136110.

Palmquist, J.C., 1978, Laramide structures and basement block faulting: Two examples from the Big Horn Mountains, Wyoming. in Matthews, V. eds. Laramide Folding Associated with Basement Block Faulting in Western United States. Geological Society of America Memoir, v. 151, p. 125-138.

Peyton, S.L., Reiners, P.W., Carrapa, B., DeCelles, P.G., 2012, Low-temperature thermochronology of the northern Rocky Mountains, western U.S.A: American Journal

of Science, v. 312, p. 145-212.

Potter, P.E., Pettijohn, F.J., 1977, Paleocurrents and Basin Analysis. Springer-Verlag, Berlin. p 550.

Rice CA, Flores RM, Stricker GD, et al., 2008, Chemical and stable isotopic evidence for water/rock interaction and biogenic origin of coalbed methane, Fort Union Formation, powder river basin, Wyoming and Montana U.S.A: International Journal of Coal Geology, v. 76, p. 76–85.

Rose, K., 1981, The Clarkforkian Land-Mammal Age and Mammalian Faunal Composition Across the Paleocene-Eocene Boundary: Papers on Paleontology. v. 26. p. 197.

Ryder, R.T., and Scholten, R., 1973, Syntectonic conglomerates in southwestern Montana: Their nature, origin, and tectonic significance: Geological Society of America Bulletin, v. 84, p. 773–796.

Santos, M. M., Lana, C., Scholz, R., Buick, I., Schmitz, M. D., Kamo, S. L., Gerdes, A., Corfu, F., Tapster, S., Lancaster, P., Storey, C. D., Basei, M. A., Tohver, E., Alkmim, A., Nalini, H., Krambrock, K., Fantini, C. and Wiedenbeck, M., 2017, A New Appraisal of Sri Lankan BB Zircon as a Reference Material for LA-ICP-MS U-Pb Geochronology and Lu-Hf Isotope Tracing. Geostand Geoanal Res, v. 41, p. 335-358. doi:10.1111/ggr.12167

Schmitt, J.G. & Steidtmann, 1990, Interior ramp-supported uplifts: Implications for sediment provenance in foreland basins: Geology, v. 102, p. 494-501.

Schmitz, B. & Pujalte, V., 2007, *Abrupt increase in seasonal extreme precipitation at the Paleocene-Eocene boundary*: Geology, v. 35, p. 215–218.

Secord, R., Gingerich, P.D., Smith, M.E., Clyde, W.C., Wilf, P., and Singer, B.S. 2006. Geochronology and mammalian biostratigraphy of middle and upper Paleocene

continental strata, Bighorn Basin, Wyoming: American Journal of Science, v. 305, p. 211-245.

Seeland, D. 1998, Late Cretaceous, Paleocene, and early Eocene paleogeography of the Bighorn Basin and northwestern Wyoming. In: Cretaceous and Lower Tertiary Rocks of the Bighorn Basin, Wyoming and Montana: 49th Annual Field Conference Guidebook, p. 1-29.

Smedes, H.W., and Prostka, H.J., 1972, Stratigraphic framework of the Absaroka Volcanic Supergroup in the Yellowstone Park Region: U.S. Geological Survey Professional Paper #729C, p. 33.

Smith, G. R., Morgan, N., and Gustafson, E., 2000. Fishes of the Mio-Pliocene Ringold Formation, Washington: Pliocene capture of the Snake River by the Columbia River. University of Michigan Papers on Paleontology 32.

Smith, J.J., Hasiotis, S.T., Kraus, M.J. & Woody, D.T., 2008, Relationship of floodplain ichnocoenoses to paleopedology, paleohydrology, and paleoclimate in the Willwood Formation, Wyoming, during the Paleocene-Eocene Thermal Maximu: Palaios, v. 23, p. 683–699.

Snell, K.E., Thrasher, B.L., Eiler, J.M., Koch, P.L., Sloan, L.C. & Tabor, N.J., 2012, Hot summers in the Bighorn Basin during the early Paleogene: Geology, v. 41, p. 55–58.

Stearns, M.T. & Stearns, D.W., 1978, Geometric analysis of multiple drape folds along the northwest Big Horn Mountains front, Wyoming. in Matthews, V. eds. Laramide Folding Associated with Basement Block Faulting in Western United States: Geological Society of America Memoir v. 151, p.125-138.

Sundell, K.A., 1993, The Absaroka volcanic province, in Snoke A.W., Steidtman, J.R. and

Roberts, S.M., eds., Geology of Wyoming: Geological Survey Memoir #5, p. 572-603.

Sundell, K.A., 1990, Sedimentation and tectonics of the Absaroka Basin of northwestern Wyoming, *in* Specht, R., ed., *Wyoming sedimentation and tectonics* : Casper, Wyoming, Wyoming Geological Association, 41st Annual Field Conference Guidebook, p. 105–122.

Steidtmann, J. R., and Middleton, L. T. 1991, Fault chronology and uplift history of the southern Wind River Range, Wyoming: Implications for Laramide and post-Laramide deformation in the Rocky Mountain foreland: Geological Society of America Bulletin, v. 103, p. 472-485.

Thewissen. J.G.M., 1990, Evolution of Paleocene and Eocene Phenacodontidae (Mammalia, Condylarthra). Univ. Mich. Pap. Paleontol., v. 29, p. 1-107.

Van Houten, J., van den Berg, A.P., and Vlaar, N.J., 2004, Various mechanisms to induce present-day shallow flat subduction and implications for the younger Earth: A numerical parameter study: Physics of the Earth and Planetary Interiors, v. 146, p. 179–194, doi:10.1016/ j.pepi.2003.07.027.

Whipkey, C.E., Cavaroc, V.V., and Flores, R.M.,1991, Uplift of the Bighorn Mountains, Wyoming and Montana – A sandstone provenance study: U.S. Geological Survey Bulletin, 1917-D, p. 1-20.

Whittaker, A.C., Duller, R.A., Springett, J., Smithells, R.A. , Whitchurch, A.L., Allen, P.A., 2011, Decoding downstream trends in stratigraphic grain size as a function of tectonic subsidence and sediment supply: GSA Bulletin v. 123, p. 1967-1382.

Wing, S.L., Harrington, G.J., Smith, F.A., Bloch, J.I., Boyer, D.M., Freeman, K.H., 2005, Transient floral change and rapid global warming at the Paleocene-Eocene boundary:

Science, v. 310, p. 993–996.

Wing, S. L., Bao, H. M., and Koch, P. L., 2000, An early Eocene cool period? Evidence for continental cooling during the warmest part of the Cenozoic, in Huber, B. T., MacLeod, K., and Wing, S. L., editors, Warm Climates in Earth History: Cambridge, Cambridge University Press, p. 197–237.

Wise, D.U., and Obi, C.M., 1992, Laramide basement deformation in an evolving stress-field, Bighorn mountain front, Five Springs area, Wyoming: American Association of Petroleum Geologists Bulletin, v. 76, p. 1586–1600.

Yuretich, R. F., Hickey, L. J., Gregson, B. P., and Hsia, Y. L., 1984, Lacustrine deposits in the Paleocene Fort Union Formation, northern Bighorn Basin, Montana: Journal of Sedimentary Petrology, v. 54, p. 836 –852.

Zachos, J.C., Lohmann, K.C., Walker, J.C.G., Wise, S.W., 1993, Abrupt climate change and transient climates during the Paleogene: a marine perspective: Journal of Geology, v. 101, p. 191–213.

Zachos, J.C., Rohl, U., Schellenberg, S.A., Sluijs, A., Hodell, D.A., Kelly, D.C., Thomas, E., Nicolo, M., Raffi, I., Lourens, L.J., McCarren, H., Kroon, D., 2005, Rapid acidification Of the ocean during the Paleocene–Eocene thermal maximum: Science, v. 308, p. 1611–1615.

FIGURES

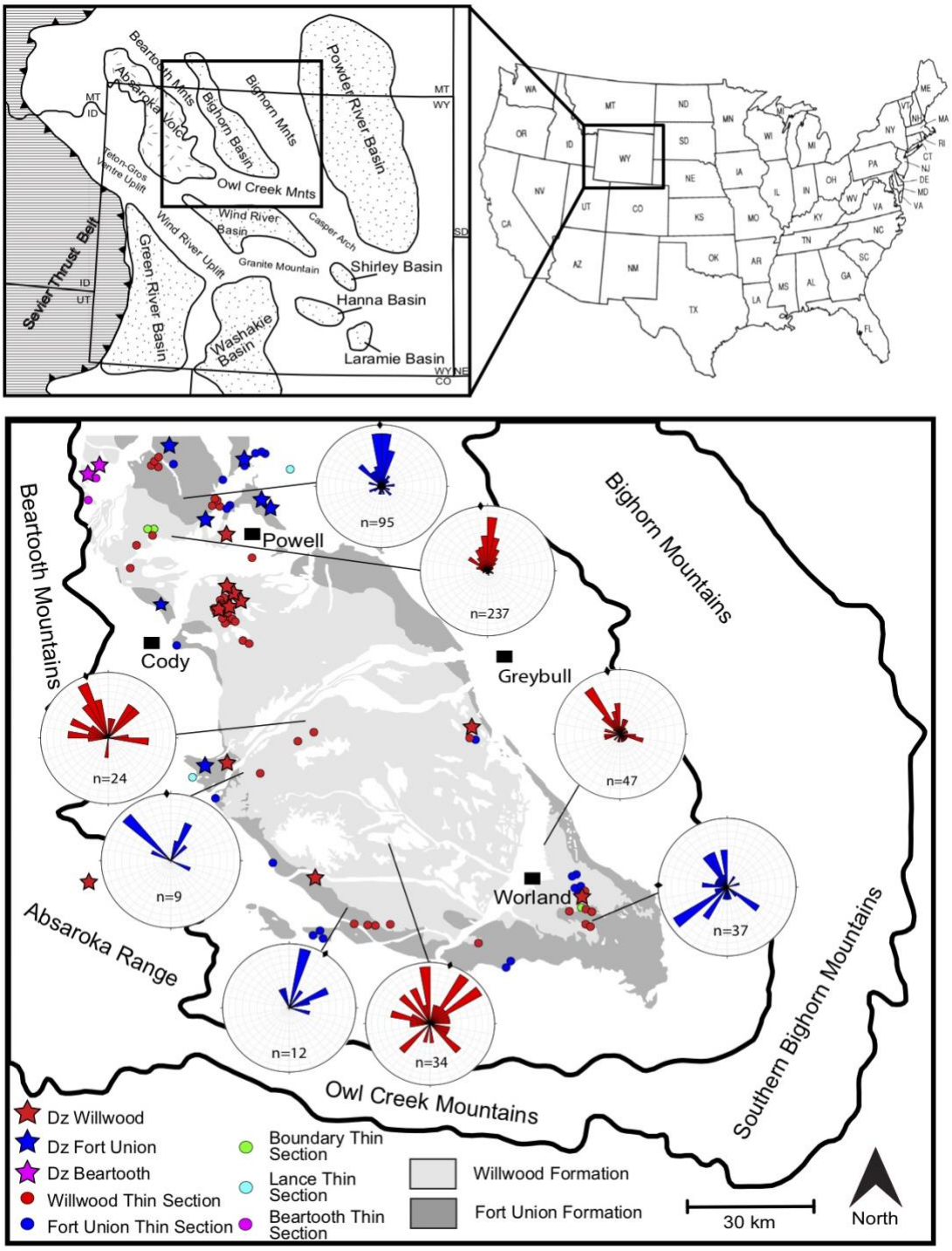

Figure 1. Geologic map of Bighorn Basin located in northwest Wyoming showing the extent of the Fort Union and Willwood formations in the basin, surrounding uplifts, location of detrital

zircon samples, thin section sample locations, and regional paleocurrent trends (this study; n = number of paleocurrent measurements and diamond the vector mean).

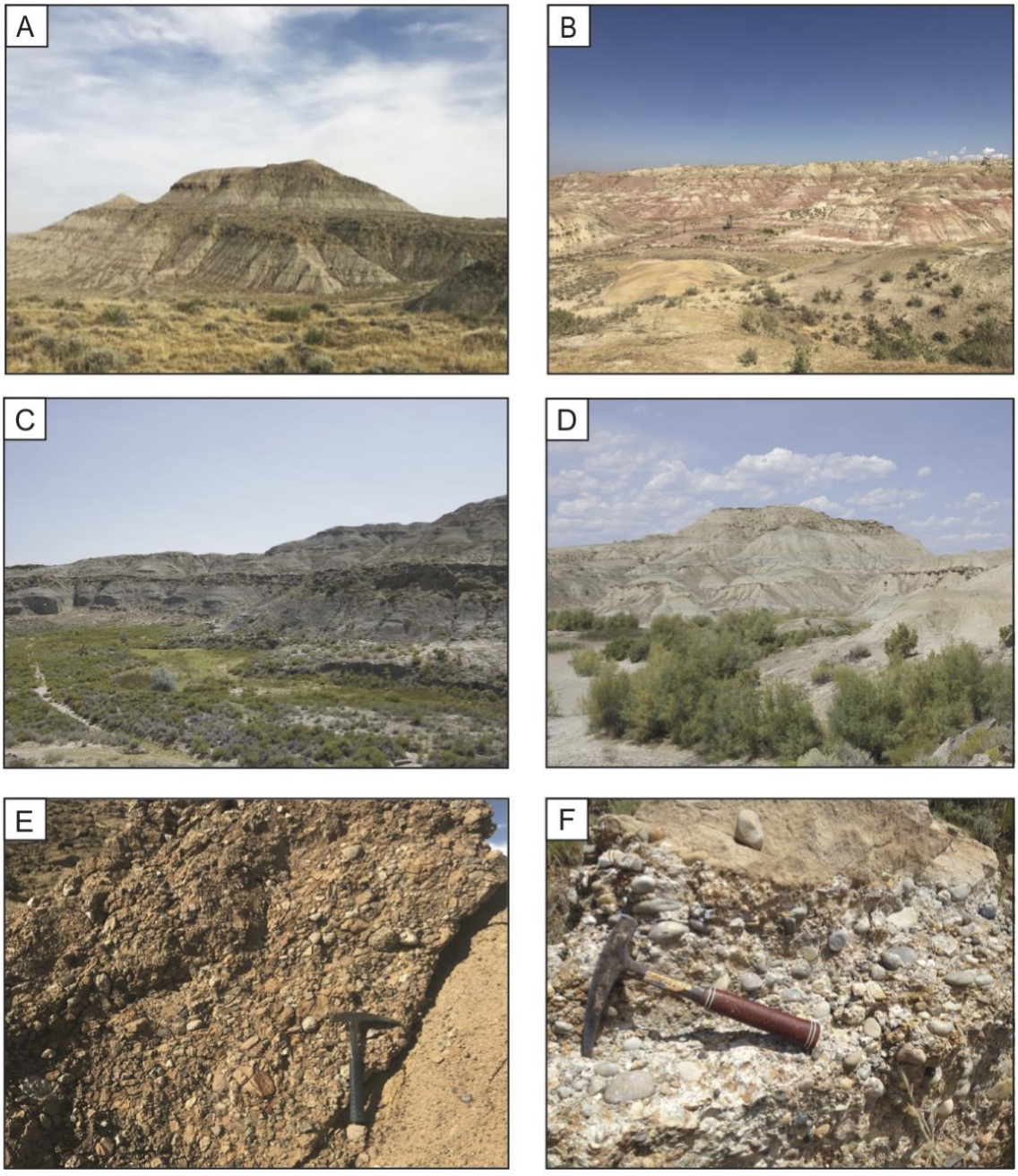

Figure 2. Outcrop photos of A) Willwood formation from the north, B) Willwood formation in the Southeast, C & D) Fort Union formation from the north, E) Beartooth Conglomerate in the north (hammer for scale), F) Willwood conglomerate in the southwest.

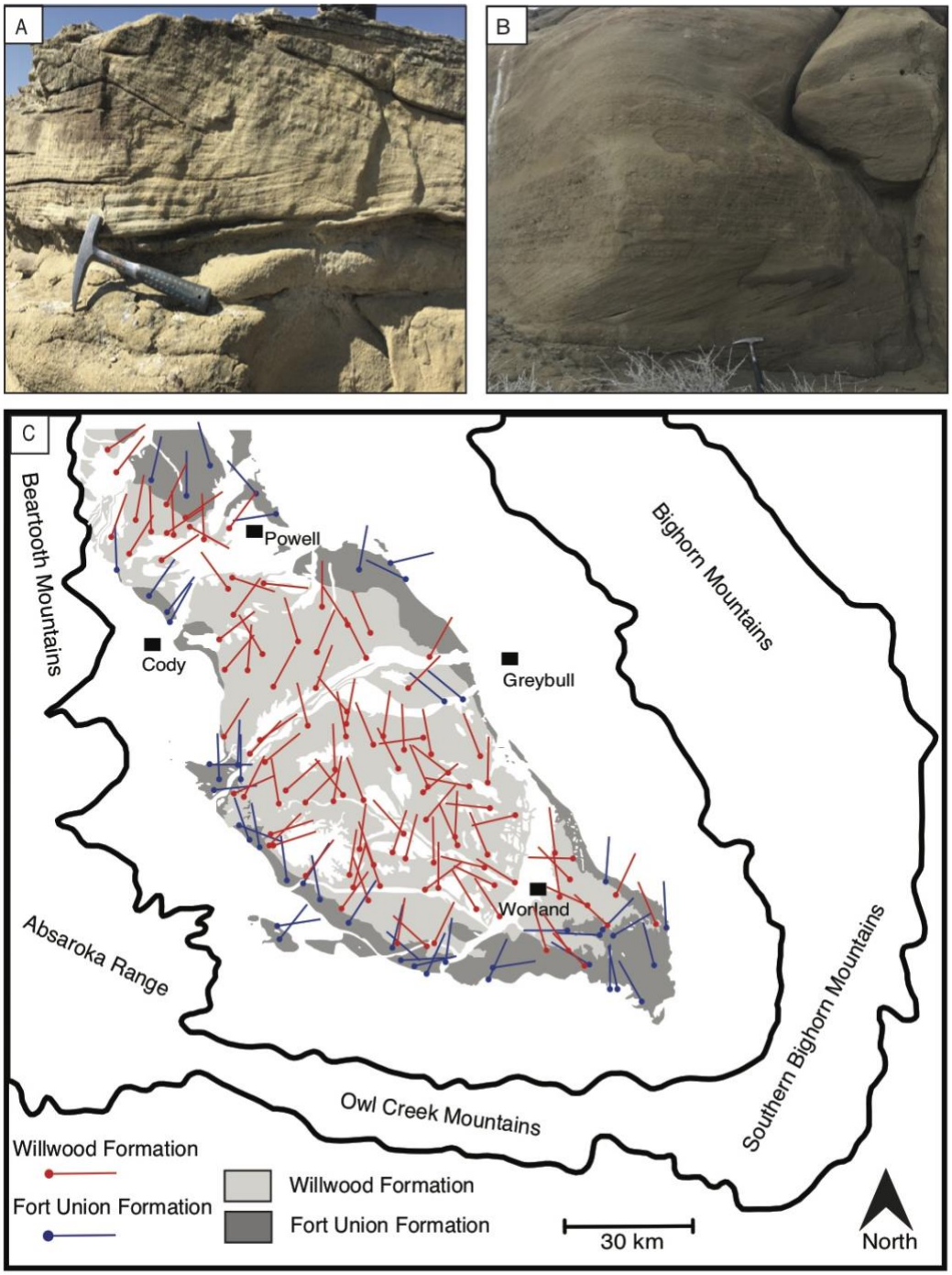

Figure 3. Field photographs of sedimentary structures used to determine the paleocurrent direction. An example of A) trough cross-bedding, and a B) trough cross-bedded unit with overlying planar bedding are shown. Both examples are from the Willwood Formation, and C) compiled vector means for paleocurrent measurements (Neasham & Vondra, 1972; DeCelles et al., 1991; Seeland, 1998; Foreman, 2014; this study).

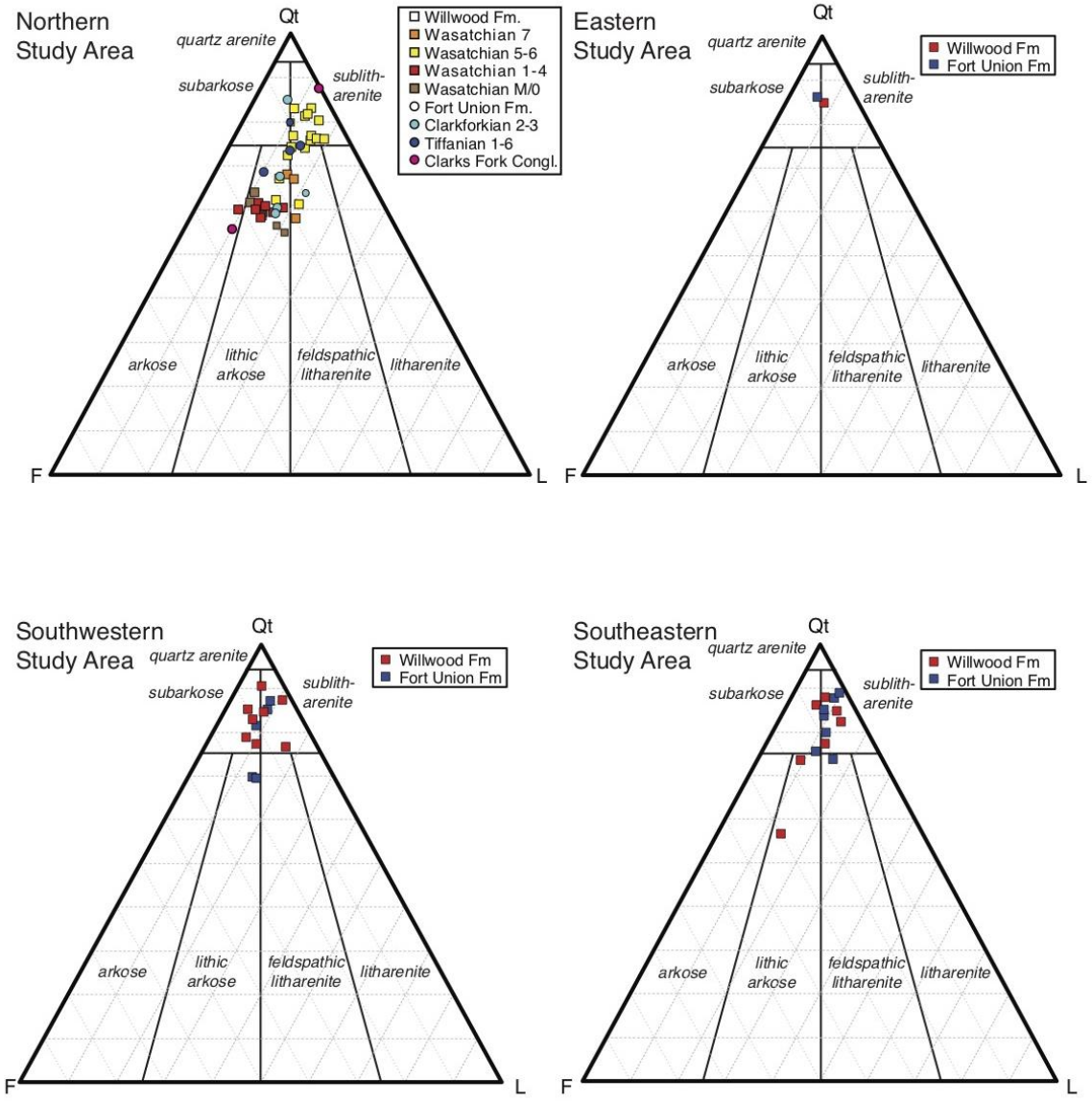

Figure 4. Point-counted sandstone, thin section data on ternary diagrams sub-divided by geographic area of study; A) northern study area, B) eastern study area C) southeastern study area D) southwestern study area. Abbreviations are Qt = total quartz, F = feldspar, and L = lithic fragments.

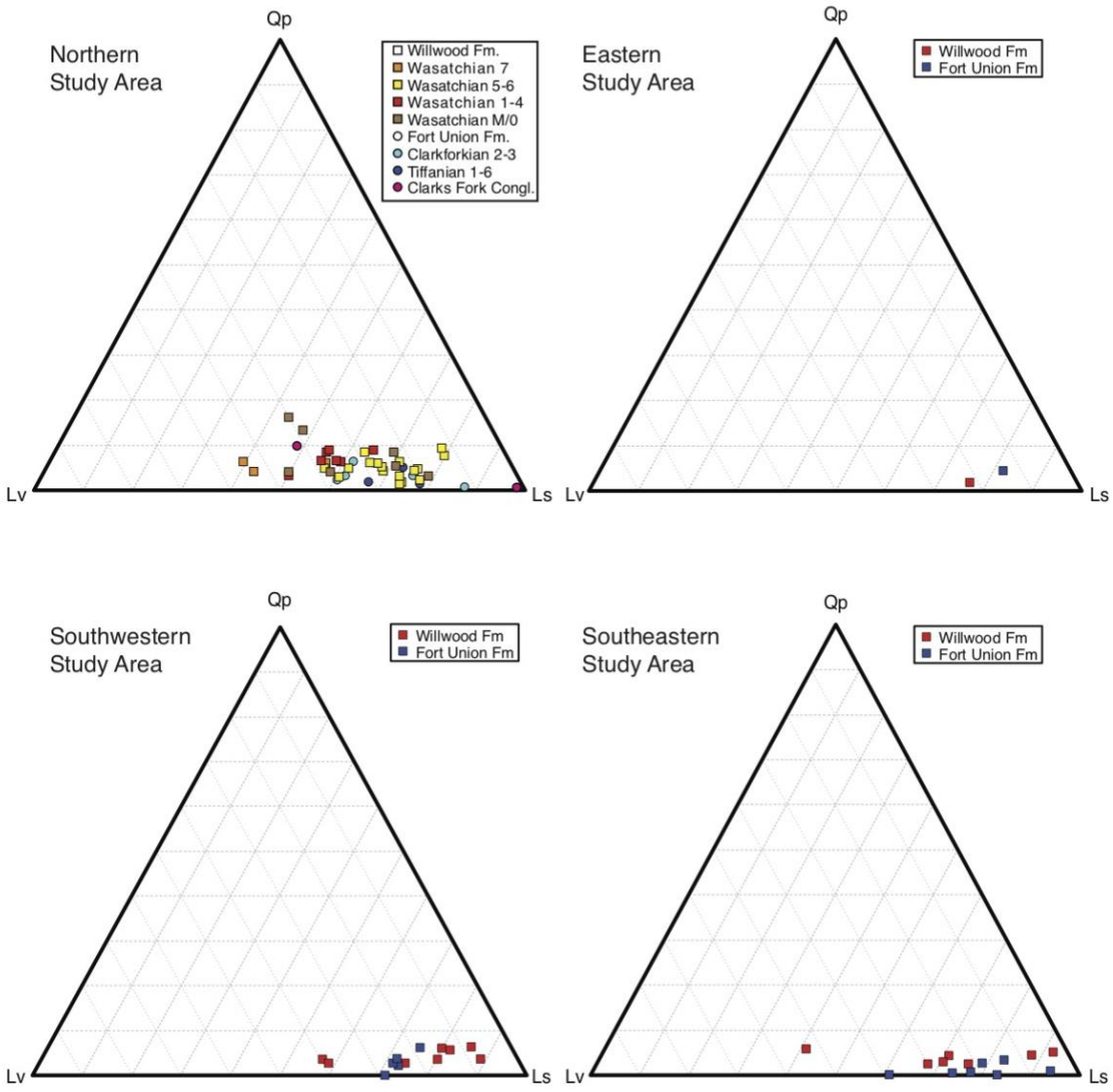

Figure 5. Point-counted sandstone, thin section data on ternary diagrams sub-divided by geographic area of study; A) northern study area B) eastern study area, C) southeastern study area, and D) southwestern study. Abbreviations are Qp = polycrystalline quartz, Ls = sedimentary lithic fragments, and Lv = volcanic lithic fragments.

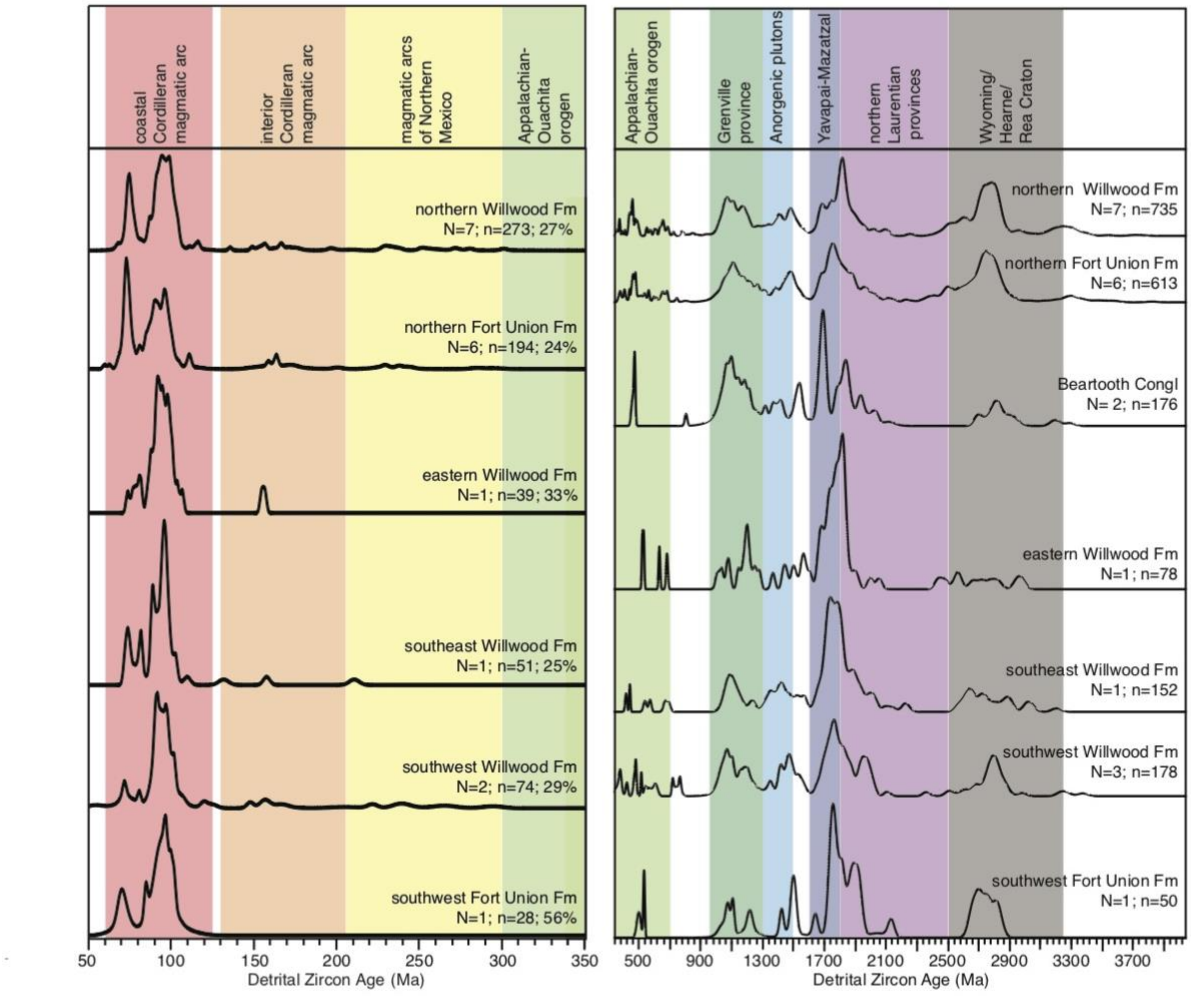

Figure 6. Detrital zircon U-Pb age spectra for the Fort Union and the Willwood formations in the north, east, southeast and southwest study areas of the Bighorn Basin. The Beartooth Conglomerate is presented but plotted separated. A) Age spectra for 0 to 300 Ma, and B) age spectra for ≥300 Ma. The Beartooth Conglomerate is only included on the ≥300 side because it has no ages less than 300 Ma.

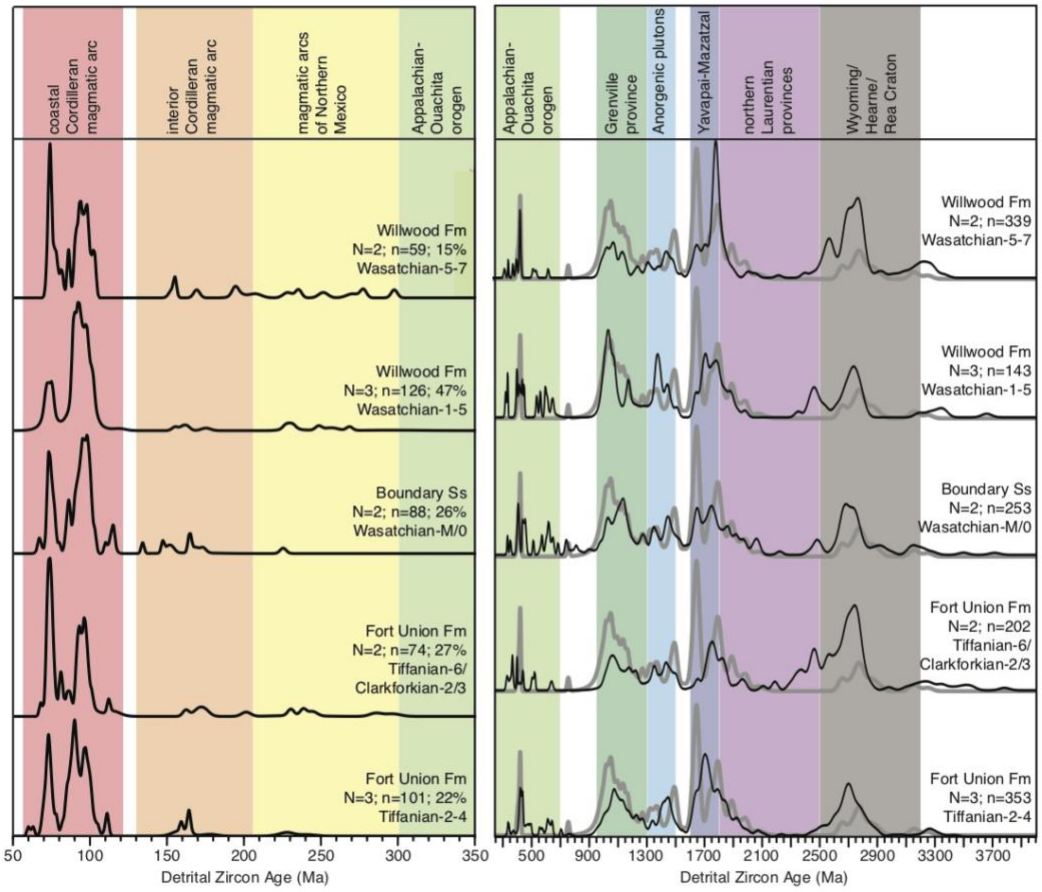

Figure 7. Detrital zircon U-Pb age spectra for the Fort Union and the Willwood formations in the northern Bighorn Basin subdivided by mammal biozone; A) Age spectra for 0 to 300 Ma, and B) age spectra for ≥300 Ma. The underlain grey curve shown for spectra ≥300 Ma is the Beartooth conglomerate.

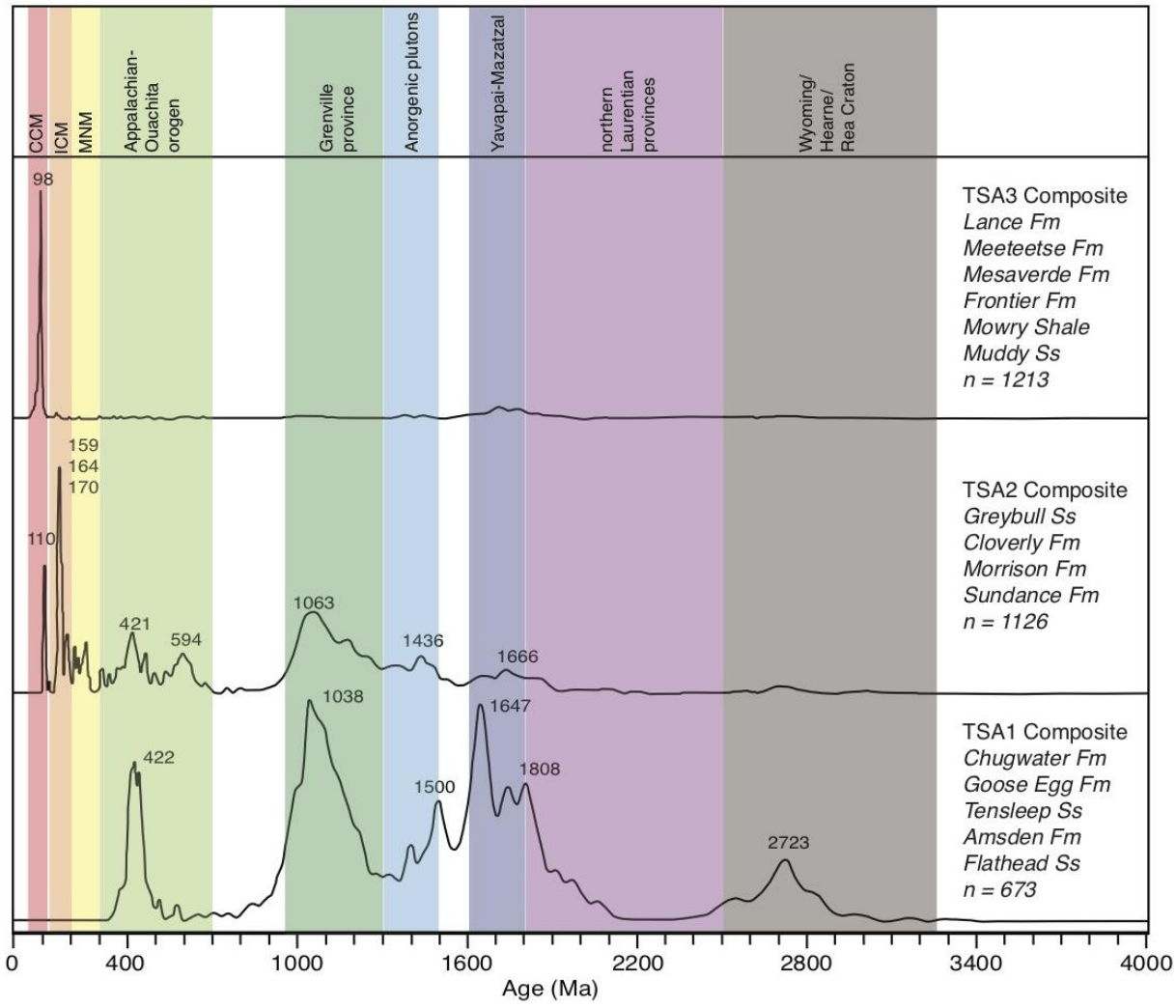

Figure 8. Detrital zircon U-Pb age spectra from sedimentary cover in Laramide uplifts surrounding the Bighorn Basin (modified from May et al., 2013).

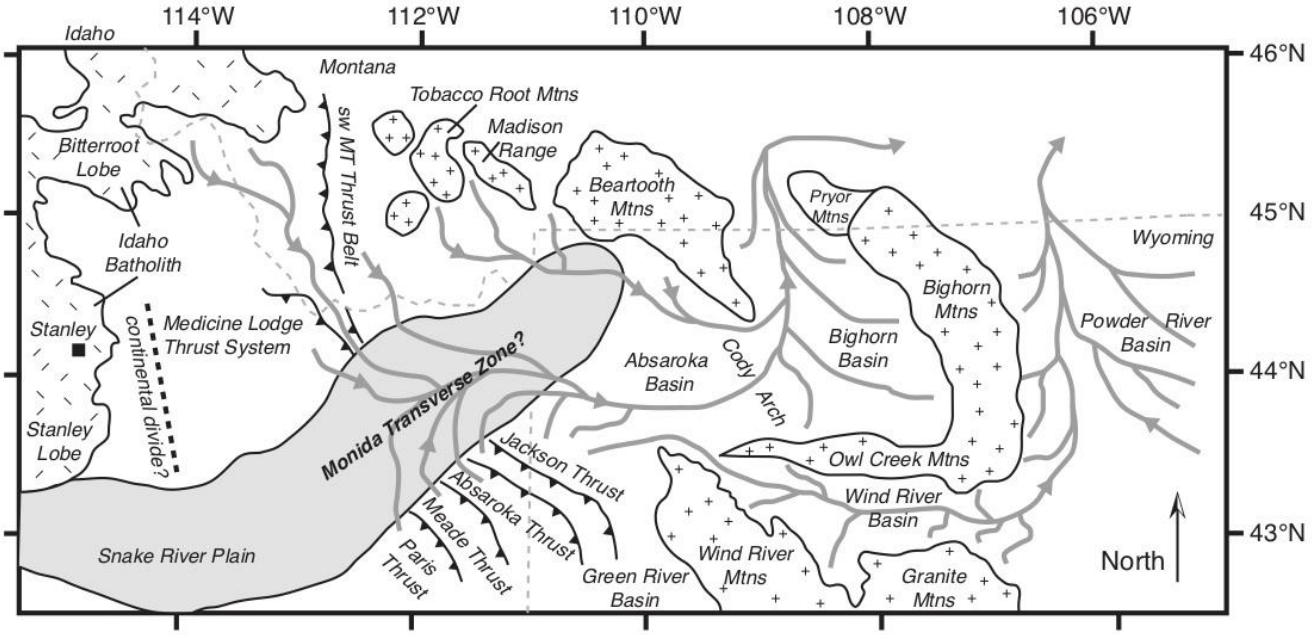

Figure 9. Paleogeographic reconstruction of Wyoming and surrounding region during the early Paleogene. Arrows mark major fluvial systems draining Sevier and Laramide highlands (modified from Seeland, 1998). Today the Snake River Plain obscures the proposed Monida transverse zone of Lawton et al. (1994) and Absaroka Volcanics cover the proposed Absaroka Basin.

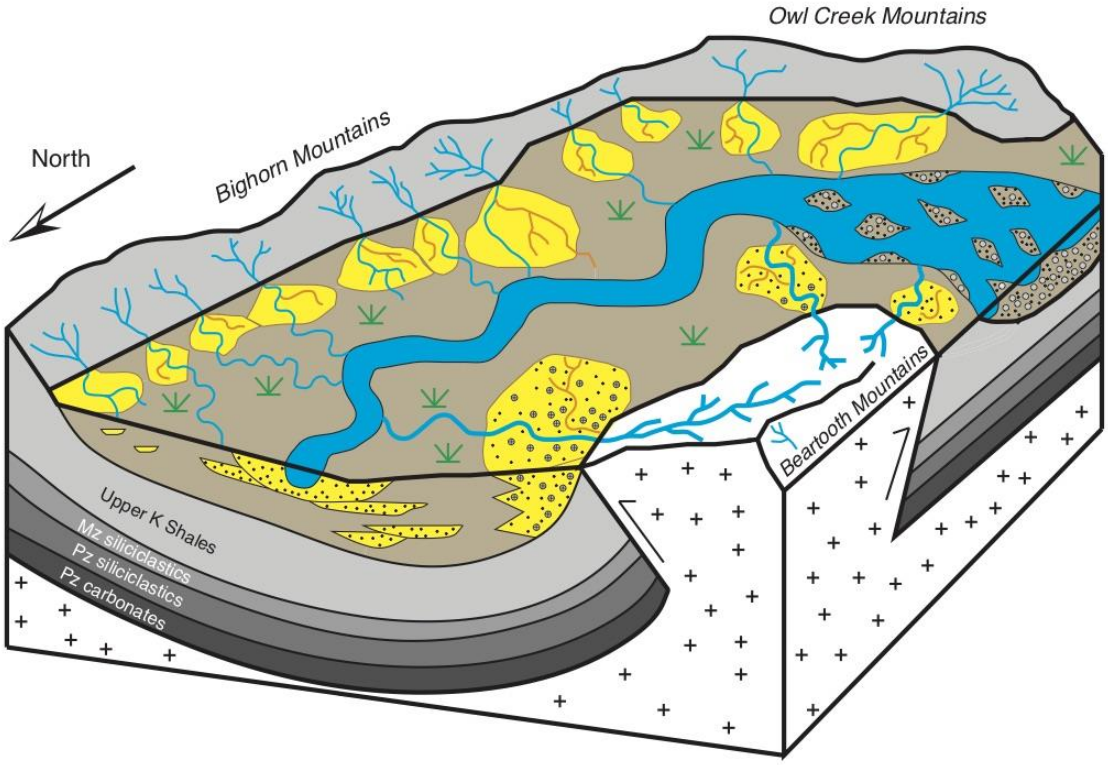

Figure 10. Schematic reconstruction of Bighorn Basin early Paleogene stratigraphy (modified from Owen et al., 2017).

Table 1. Summary of grain composition for study areas. Shown are mean percentages for each with one standard deviation from the mean (± 1σ). N = the number of thin section in each group, n = the number of points counted.

	Total Quartz (Qt)	Felds-par (F)	Lithics (L)	Monocrys-talline Quartz (Qm)	Plagioclase (P)	Orthoclase (K)	Polycrys-talline Quartz (Qp)	Sedimentary Lithic Fragments (Ls)	Volcanic Lithic Fragments (Lv)
East Willwood Fm (N=1;n=502)	85%	7%	8%	85%	5%	11%	2%	76%	22%
East Fort Union Fm (N=1;n=504)	86%	8%	6%	84%	3%	14%	5%	82%	14%
Southeast Willwood Fm (N=6;n=3016)	82% ± 6	8% ± 5	10% ± 3	81% ± 14	2% ± 1	17% ± 13	4% ± 1	77% ± 10	19% ± 11
Southeast Fort Union Fm (N=7;n=3524	82% ± 6	7% ± 4	11% ± 3	84% ± 9	2% ± 1	14% ± 8	1% ± 1	79% ± 10	20% ± 10
Southwest Willwood Fm (N=8;n=4035)	83% ± 5	8% ± 4	9% ± 4	79% ± 11	5% ± 5	16% ± 9	5% ± 2	76% ± 12	20% ± 13
Southwest Fort Union Fm (N=5;n=2545)	79% ± 8	11% ± 6	11% ± 3	77% ± 11	6% ± 5	17% ± 6	3% ± 2	73% ± 1	24% ± 4
North Willwood Fm (N=34,n=16941)	68% ± 9	17% ± 9	15% ± 3	67% ± 15	15% ± 8	18% ± 8	6% ± 3	63% ± 11	31% ± 10
North Fort Union Fm (N=9,n=4503)	70% ± 9	16% ± 6	14% ± 5	71% ± 9	12% ± 6	17% ± 3	3% ± 2	70% ± 9	26% ± 8
Beartooth Conglomerate (N=2,n=1016)	72% ± 22	17% ± 23	12% ± 1	71% ± 40	16% ± 22	13% ± 18	5% ± 6	22% ± 28	73% ± 35

Table 2. List of major detrital zircon U-Pb age peaks and relative abundance of grains that fall within each primary source age range by sample.

	coastal Cordilleran magmatic arc (CCM)	interior Cordilleran magmatic arc (ICM)	magmatic arcs of Northern Mexico (MNM)	Appalachian-Ouachita orogen (AOO)	Grenville Province (GP)	Anorogenic Plutons (AP)	Yavapai-Mazatzal (YMP)	northern Laurentian provinces (NLP)	Wyoming/ Hearne/ Rea Craton (WHR)
Major Age Peaks Identified									
Northern Willwood Fm	75, 87, 96, 98, 117	–	–	334, 415, 621	1070, 1180	1483	1692, 1743	1820	2796, 3248
Northern Fort Union Fm	74, 93, 97, 113	166	–	439, 634	1105	1485	1743	1933, 2459	2746, 3297
Beartooth Conglomerate	100	–	–	436	1063, 1153, 1286	1387, 1507	1655	1807, 1908, 2002	2680, 2790,3164
Eastern Willwood Fm	75, 82, 93, 97, 106	157	–	491, 609, 644	1025, 1069, 1186	1355, 1443-1532	1692-1792	1949,2025, 2436	2538, 2929
Southeastern Willwood Fm	75, 81, 90, 96	160	–	396, 404, 539, 652	1095	1424	1734, 1794	1857, 1935, 2204	2621, 2866,3006
Southwestern Willwood Fm	69, 85, 93, 98, 102	–	–	344, 442, 478, 577, 716, 732	1069, 1190	1422, 1483	1774	1962	2794
Southwestern Fort Union Fm	72, 86, 97	–	–	468, 495	1061, 1102, 1224	1424, 1494	1643, 1769	1899, 2146	2694, 2812